

# Conceptual design of a climate neutral regional airliner

Group 7

*Students:*

J. LEEFTINK S2188295  
M. LAMERS S1935429  
R. KOENDERINK S2139995  
H. JEKEL S1802178  
D. TJOKROSETIO S2089688  
N. JANSEN S2184745  
S. E. F ISMAIL S2169851  
M. SCHNATTERER S2621150

*Module coordinator:*

dr.ir. E. van der WEIDE

June 26, 2024



# Contents

<b>1</b>	<b>Introduction</b>	<b>2</b>
<b>2</b>	<b>Requirements and Technical Specifications</b>	<b>2</b>
<b>3</b>	<b>Concept Generation</b>	<b>2</b>
3.1	Elements of the aircraft . . . . .	3
3.2	Final concept . . . . .	4
<b>4</b>	<b>Design</b>	<b>4</b>
4.1	Mass estimation . . . . .	4
4.2	Flight envelope . . . . .	5
4.3	Performance . . . . .	5
4.4	Fuselage design . . . . .	7
4.5	Stabilizer design . . . . .	9
4.6	Landing gear design . . . . .	10
4.7	Wing design . . . . .	11
4.8	Engine Design . . . . .	15
<b>5</b>	<b>Evaluation and Conclusion</b>	<b>16</b>
	<b>Bibliography</b>	<b>17</b>
	<b>Appendix A Requirements</b>	<b>20</b>
	<b>Appendix B Fuselage drawings</b>	<b>21</b>
	<b>Appendix C Business Case</b>	<b>22</b>
C.1	Problem . . . . .	22
C.2	Solution . . . . .	22
C.3	Value . . . . .	23
C.4	Market size and future development . . . . .	23
C.5	Competition and possible partners . . . . .	24
C.6	Competences and Complexity . . . . .	24
C.7	Uncertainty . . . . .	25
C.8	Costs and returns . . . . .	25
C.9	Times . . . . .	26
C.10	Risks . . . . .	26
	<b>Appendix D Group contribution</b>	<b>27</b>
	<b>Appendix E Fact sheet</b>	<b>28</b>

# 1 Introduction

The project group is hired by *Twente In The Air Netherlands* (TITAN) to develop a climate-neutral regional airliner for Airbus. This report describes the conceptual design for this aircraft. Firstly, requirements are established based on the demands of TITAN and Airbus. Since not only the engineering viewpoint is of importance, but also the financial aspect, a business case is formed from which requirements originated as well. Thereafter, the concept generation is done in which design choices are made. These choices are often interrelated and rely on the stated requirements. The final concept is elaborated on concerning airworthiness, feasibility and predicted performance. In the end, a well-considered conceptual design is presented that meets the requirements and demands of TITAN and Airbus.

## 2 Requirements and Technical Specifications

The requirements for the concept design of this specific aircraft have partially been established by TITAN and Airbus. Furthermore, a business case (Section C) was made in order to analyze the economical and technical feasibility of an aircraft restricted by those requirements. Based on the business case, a specific target market was selected to possibly deploy the aircraft to. Based on this market and its requirements, additional requirements for the aircraft were composed.

In Table 9, these requirements can be found. These requirements are quantified (between brackets) where possible. Furthermore, the improvement score is shown on a scale from 1 to 5. A score of 1 means the criteria can't be improved upon and a 5 means that a lot can be improved. The table with the requirements can be found in Appendix A.

As seen in Table 10, Appendix A, safety is the most important factor during the design. However, this should be done in the cheapest way possible, since costs are of major importance. Furthermore, it is vital that the aircraft can operate at most airports; i.e. the required runway length is not too high and the aircraft can operate at most gates. Finally, the passenger's comfort has to be taken into account. Furthermore, some requirements/assumptions from TITAN and Airbus have to be taken into account:

1. The plane should be compatible with the Flight Path 2050 targets regarding improved mobility, emissions and economic efficiency.
2. When combustion engines are used in combination with hydrogen, the engine performance can be assumed to be the same as for fossil fuels. However, the actual storage of hydrogen will require attention. This is also the case when fuel cells are used.
3. When batteries are used the energy density of batteries can be taken 1.5 times the current state of the art, as it will take some time before this aircraft will actually fly.
4. Direct operating costs should be as low as possible. Unless otherwise indicated, extra performance does not increase chances of winning the design contest; low cost does.
5. There are no restrictions on engine type selection (ducted fan, propellers), nor on the number of engines allowed to be used, as long as the propulsion is climate neutral.
6. Parts of the aircraft that need more than minor repairs should be easily removable.

These requirements and the requirements in Table 9 should be taken into account during the concept generation phase. Furthermore, the importance of these requirements according to Table 10 should be kept in mind.

## 3 Concept Generation

In this section, the concept is elaborated based on the requirement rating of Chapter 2. Table 1 displays the morphological diagram generated during the concept generation phase. From this table, two concepts were divided into hydrogen and electrical concepts. In Table 1, pink represents the electric concept and green represents the hydrogen concept. In case an element is chosen for both concepts it is also made green. Instead of discussing both concepts, only the chosen concept will be elaborated on in Section 3.1.

	Solution A	Solution B	Solution C	Solution D	Solution E
Propulsion	Distributed	Few engines			
Configuration	Tandem	Canard	Conventional	Box	
Wing placement	Blended wing	Below the fuselage	Above the fuselage	Middle of the fuselage	
Stabilizers	Cruciform	T-tail	V-tail	Conventional	
Passenger entry	Top of the fuselage	Bottom of the fuselage	Side of the fuselage	Back of the fuselage	Front of the fuselage
Fuel	Hydrogen combustion	Hydrogen fuel cell	Batteries	Hybrid	
Seat class	All business class	All economy	Combination		
Engine type	Piston Propeller	Turboprop	Turbofan	Turbojet	Electric propeller
Engine placement	Pusher	Tractor	Both		
Landing gear	Taildragger	Bicycle	Tricycle		
Vision for passenger	Windows	Camera			
Location of engines	Front of the wing	Back of the wing	On the tail of fuselage		
Wing sweep angle	Straight	Swept back	Swept forward		
Wing dihedral angle	Dihedral	Anhedral	Polyhedral		

Table 1: The morphological diagram

### 3.1 Elements of the aircraft

#### Energy source

Fuels that are considered most reliable and achievable are batteries, hydrogen and hybrid of these two. In Table 2, important characteristics of hydrogen and batteries are compared for aircraft applications. A green color means favorable, a red color means unfavorable and a yellow color means in between.

	Hydrogen	Batteries
Energy density	120MJ/kg	0.36-0.95 MJ/kg
Costs	Expensive cf.	Cheap cf.
Future expectations	Costs will reduce	Degenerate over time
Dangers	Explosive	Short circuit, fire hazard
Ground procedure	Refill as usual	Need to be replaced
Space/Volume	Stored at low T and P=1.5bar [1]	Many batteries, heavy
Efficiency	Comparable to kerosine	Much higher than kerosine

Table 2: Comparison of key characteristics of hydrogen and batteries.

Hydrogen has a high energy density and allows the existing ground and maintenance procedures to stay, maybe with some slight adaptations. Direct combustion only requires storage of the fuel while fuel cells require more space and adds weight. Additionally, the hydrogen prices are expected to lower in the future. Therefore the aircraft will be fueled by direct hydrogen combustion.

#### Engine choices

The engine options for the required flight performance are a turboprop, a prop-fan, a turbofan and a turbojet[2]. From these options, the turboprop is the most affordable engine, with the best take-off performance and the lowest specific fuel consumption. Despite the turboprop being more complex engine compared to the other options, the operating costs of this engine are still lower than for the other engines. The turboprop is capable of operating at 9000m [2], therefore the most suitable engine option for this conceptual design is a turboprop. Since larger turboprops have a higher power to weight ratio than smaller ones, it is more beneficial to have two powerful turboprops than four or less powerful turboprops from a weights perspective. These engines should both power one propeller, since this is more efficient than powering multiple propellers with a single engine [3]. Engine placement on the wing in a pulling configuration is the most suitable option. This way, the propeller can operate in undisturbed air, increasing efficiency. This is needed since thin air at 9000 m causes a reduction in available power. Also, the engine noise in the cabin and the bending moment in the wing during flight is reduced by placing the engines on the wings. Furthermore, the pulling configuration is more stable compared to the pushing, thus the size of the vertical stabilizer can be reduced in comparison with a pushing configuration. The propellers can also be mounted in front of the wing in a pulling configuration. The landing gear can be smaller, thus requiring less space and weight [3].

#### Wing configuration

A tandem configuration was discarded due to aerodynamic losses caused by the small aspect ratio and an increase of tip vortices. Although the canard configuration can have excellent stalling characteristics and pitch response, it has some disadvantages concerning the lift coefficient. It also implies disadvantages with respect to space. The blended wing is especially useful for large aircraft and therefore not suitable for our design. The boxed wing does not seem feasible since there are no current real boxed wing designs. The conventional configuration seems to be favourable for these reasons. The wing under the fuselage increases taxiing stability by reducing the take-off distance and the landing gear can be placed in the wing. Since this configuration is also commonly used in today's commercial aircraft, this configuration was chosen. To increase the stability during flight, a dihedral configuration will be used.

## Tank position

Due to the cylindrical shape that the hydrogen tank needs to have, the positions are limited. Therefore the main positions that are considered are under the wings, in the back, on top and at the bottom of the aircraft. The tank on the bottom is not favourable due to safety reasons. The safety of the remaining positions is similar. The chances of survival are low for any of other options in case something goes wrong in-flight, hence the position should be based on the performance. Various performance aspects were analyzed; firstly the influence on the performance by the positional change of the centre of gravity; secondly the influence on aerodynamics, and lastly the influence on the hydrogen boil-off. The tank on top of the aircraft appears to be the most efficient [1; 4], therefore it is chosen as the tank's position.

## Stabilizer

The conventional configuration offers simpler mechanics and fewer weight implications than the T-, V- and cruciform tails. However, it may have problems in the engine wake. The advantages of the conventional configuration are more preferable, so this configuration is chosen.

## Landing gear

The tricycle landing gear is the most suitable for conventional aircraft due to high stability, good visibility from the flight deck, forceful braking, prevention of ground-looping, horizontal cabin and good take-off rotation [5]. A fixed landing gear is typically less complicated, cheaper and lighter than retractable gears, but increase drag and weight significantly [6]. When the aircraft reaches a cruise velocity of 150 knots (77.17 m/s), a retractable landing gear is beneficial [7]. This is applicable for this conceptual aircraft.

## Passenger vision

Excluding windows in the aircraft can reduce the weight and increase safety [8]. Glass is heavy, can need reinforcement and introduces stress concentrations to the fuselage. To give passengers a view of the outside, display-screens and cameras can be used. Besides the reduction of the aforementioned risks, the airliner could display other content on the screens [9]. Therefore, display-screens and cameras were opted for instead of windows.

## 3.2 Final concept

To summarize the above, Table 3 was made. At the front page of the report, the concept is shown.

Table 3: Final Concept

<b>Propulsion</b>	Hydrogen combustion
<b>Engine type</b>	Turboprop
<b>Engine placement</b>	Tractor
<b>Wing configuration</b>	Conventional
<b>Wing position</b>	Dihedral low wing
<b>Tank position</b>	On top of fuselage
<b>Stabilizer</b>	Conventional
<b>Landing gear</b>	Tricycle
<b>Passenger vision</b>	Display-screens

## 4 Design

### 4.1 Mass estimation

In the positioning of the masses along the fuselage, the masses are taken as point masses for simplicity. This is also done in the fuselage structural analysis. The masses and position of centre of mass are shown in Table 4.

Table 4: Mass estimation of the aircraft [10] [11]

Name	Mass[kg]	Position[m]	Name	Mass[kg]	Position[m]
m_frontbulkhead	18.75	1	m_furniture	1868.56	13.275
m_oxygen	129.6	5.9	m_paint	141.56	13.275
m_airco+antiice	512.32	5.9	m_fuselage	3527	13.275
m_instrument	61.18	5.9	m_landinggear	823.51	15.15
m_nosewheel	171.69	6.65	m_wing	4342.3	15.15
m_frontcargofloor	47.2	11.35	m_rearcargofloor	29.85	18.4
m_tank	360.77	12.41	m_rearbulkhead	82.87	20.65
m_nacelle	313.9	12.9	m_tail	610.26	23.6
m_propulsion	1660.5	12.9	m_apu	53.75	23.6
		<b>Total:</b>	OEW	14074.1	x

	Name	Mass[kg]	Position[m]	Name	Mass[kg]	Position[m]
	OEW	14074.1	x	MZFW	32594.1	x
	m_cargo1	1000	11.35	m_fuel	839	12.41
	m_crew	390	13.275			
	m_passengers	7470	13.275			
	m_cargo2	660	18.4			
<b>Total:</b>	MZFW	23594.1	x	MTOW	24433.1	x

The position of the tank is chosen based on the position where the change in center of gravity for a full or empty tank is minimal and remains in front of the aerodynamic center. This means that the center of gravity is at 13.84 m from the nose for a full tank and 13.91 m for an empty tank.

## 4.2 Flight envelope

The flight envelope in Figure 1 shows the V-n diagram, which plots the load factor against the flight speeds.

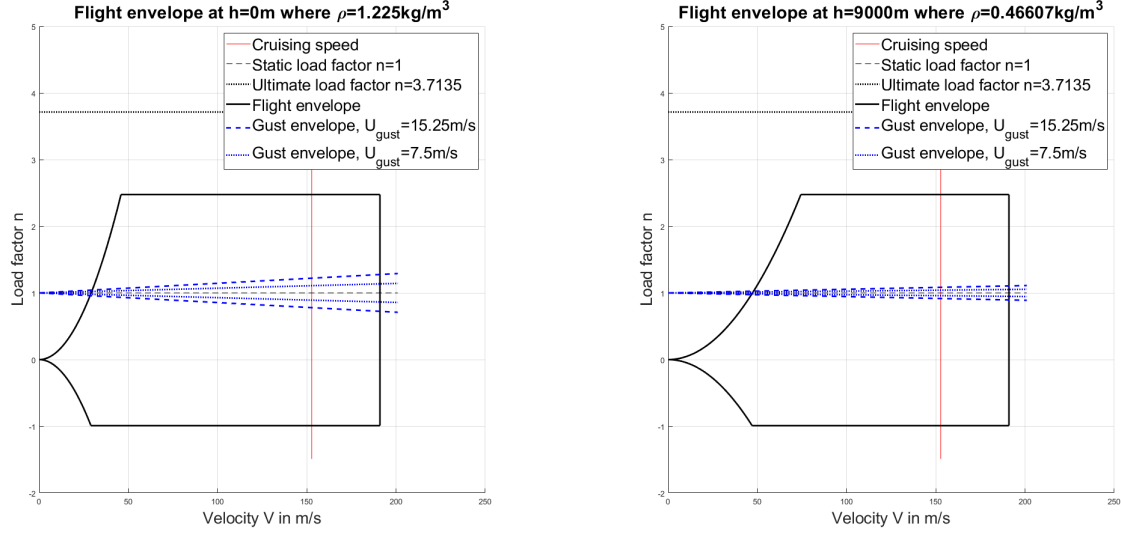


Figure 1: Flight envelopes with gust envelopes at 0m and 9000m altitude.

The top part of the diagram is defined with a positive limit load factor determined by Equation 1 [12; 13], where W is the aircraft weight in lbs[13].

$$n_1 = 2.1 + \frac{24000}{W + 10000} = 2.48 \quad (1)$$

$$n = 1 + \frac{\frac{1}{2}\rho_0 V_E \frac{\partial C_L}{\partial \alpha} F u_E}{W/S} \quad (2)$$

The negative limit load factor is determined by  $n_3 = -0.4n_1 = -0.99$  [12]. The positive and negative curves on the left are determined by  $n = L/W$ , where lift coefficients  $C_{L,max}$  and  $C_{L,min}$  in cruising condition are used respectively. The right limit is the design dive speed defined as  $V_D = 1.25V_C$  [14]. The ultimate load factor  $n_{ult} = 1.5n_1$  [13; 15] is shown in Figure 1. The gust envelope is defined by Equation 2 [15; 16], where  $F = \frac{0.88\mu_g}{5.3+\mu_g}$  and  $\mu_g = \frac{2(W/S)}{\rho_0 g c_{mean} \frac{\partial C_L}{\partial \alpha}}$  [16] and  $V_E$  and  $u_E$  are the equivalent airspeed of the aircraft and gust respectively. The tested gust speeds are typical values [15].

## 4.3 Performance

The aircraft should have a range of 1000 km at most. A minimum range of 800km was chosen. It should cruise at a velocity of at least 550 km/h at an altitude of at least 9000 m. The plane should have diversion capabilities of 10% of the range and flying time. The ascent and descent trajectories have to be 7.5° and should not lead to 5% extra runway length if compared to a trajectory of 4°. To be able to take-off and land on most runways, the aircraft should take off and land within 1500 m.

**Range and Diversion Capabilities** To test the aircraft on the range and endurance requirements, the fuel consumption has been approximated numerically. The fuel burnt during liftoff is calculated by multiplying the energy used with energy density of hydrogen;  $(120 MJ/kg)^{-1}$ . The energy used for liftoff was calculated by taking the worst case scenario w.r.t. power use into account. The time to liftoff was calculated with the runway length and the average velocity during liftoff, which is calculated to be 70% of the liftoff velocity with Equation 7 [17].

During the ground roll, weight loss is not taken into account, since it takes only a small amount of time to take off. However, the total weight of the fuel burnt during the ground roll is calculated after take-off and subtracted from the initial weight in order to determine the weight of the aircraft just after lift off. During climb, the weight

loss due to fuel consumption was taken into account by recalculating the weight for every meter gained in altitude. The energy used is calculated by taking the engine output power and time steps in climb and taking chemical and gearbox efficiencies into account. The equation for the rate of climb is given by Equation 3, and the results for different altitudes are shown in Figure 3.

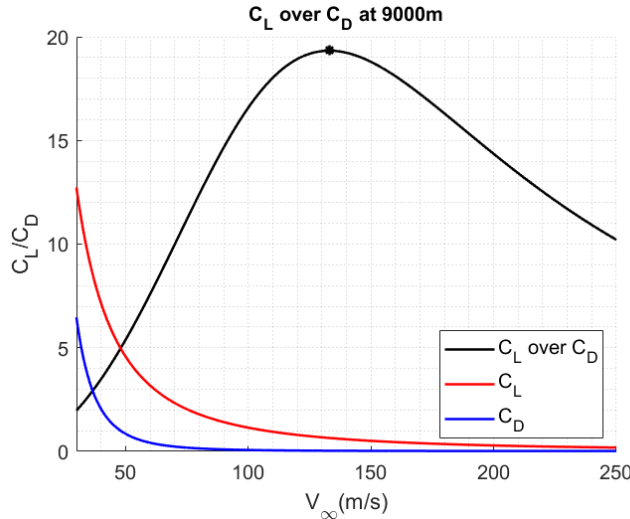


Figure 2: Aerodynamic efficiency at cruising altitude

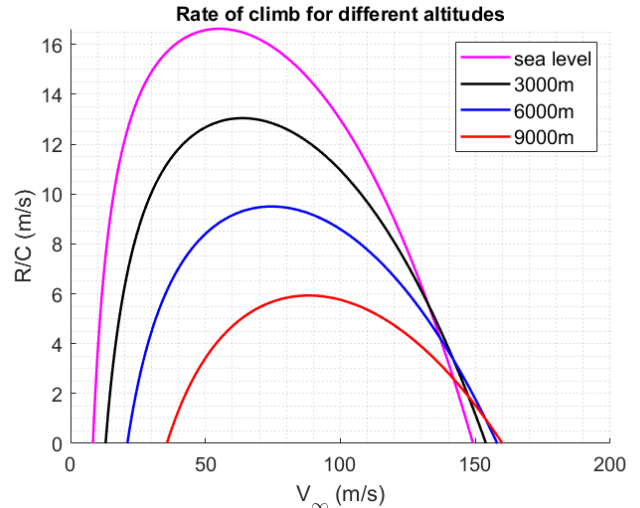


Figure 3: Rate of climb for different altitudes

The  $P_{available}$  and  $P_{required}$  can be calculated with Equation 4 and 5 respectively. The result at sea level and at cruising altitude have been plotted in Figure 4. The fuselage drag is approximated by means of a turbulent flow over a flat plate. It was found that irrespective of the engine effort, the amount of fuel used to reach cruising altitude would be constant. The factors that differ however, are the distance covered horizontally and the time to reach altitude. The distance covered during climb can be found in Figure 5.

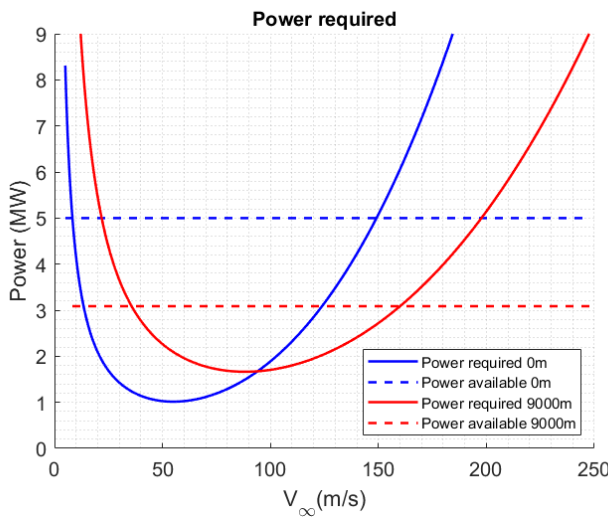


Figure 4: Power required at sea level and cruising altitude

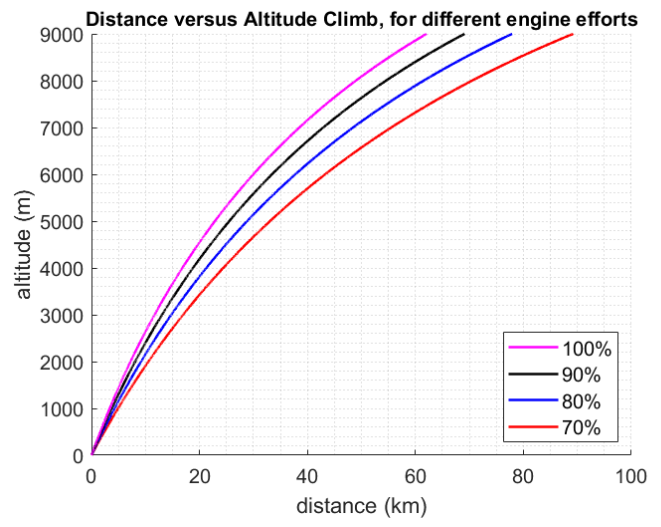


Figure 5: Distance covered during climb

$$R/C = \frac{P_{available} - P_{required}}{W} \quad (3)$$

$$P_{available}(h) = P_{engine}\eta_{propeller} \sqrt{\frac{\rho(h)}{\rho_0}} \quad (4)$$

$$P_{required} = D_{tot}V_\infty = \frac{1}{2}\rho_\infty V_\infty^3 C_{D,0} + \frac{W^2 / (\frac{1}{2}\rho_\infty V_\infty S_{wing})}{\pi e AR} + \rho_\infty V_\infty^3 C_f S_{fuselage} \quad (5)$$

The calculated energy used during cruise is based on the aircraft's changing weight. The aerodynamic efficiency during cruise is 18.66, which is close to the maximum aerodynamic efficiency at cruising altitude of 19.33 for a velocity of 133 m/s (see Figure 2). While descending, the aircraft is assumed to consume as much fuel as during cruise. To be allowed to fly by ICAO regulations when the Instrument Flight Rules (IFR) apply, the aircraft should be able to make a missed approach, fly an additional 300 km and carry an extra 5% of the planned trip fuel, to account for uncertainties. Also, a headwind of 23 m/s is taken into account. Approximately 6% of the trip fuel is used during taxiing [18]. With all this taken into account, the total estimated fuel required to be allowed to fly a minimum of 800 km is 839 kg.

**Runway Length** The engine power has been calculated based on the required runway length for lift-off by means of Equations 6 and 7. Therefore the aircraft will always be able to take off within 1500 m. However, since the engine is slightly more powerful than required, the runway will be shorter. Under normal conditions the aircraft is able to lift off in 1260 m.

$$s_{LO} = \frac{1.44W^2}{g\rho_\infty SC_{L,max}(T - [D + \mu_{asphalt}(W - L)]_{0.7V_{LO}})} \quad (6)$$

$$m\frac{dv}{dt} = -T_R - D - \mu_r(W - L) \quad (8)$$

$$V_{LO} = 1.2V_{stall} \quad (7)$$

$$V_T = 1.3V_{stall} \quad (9)$$

The force balance to find the landing distance is described by Equation 8 and the touchdown velocity by Equation 9 and the take-off lift coefficient. During touchdown, the spoilers are deployed so that lift coefficient is negligible and the zero lift drag is increased by 10% [17]. Furthermore, the brake coefficient is 0.2 for normal conditions. With these data, the landing distance can be calculated numerically for every time step. Without using reverse thrust during ground-roll in landing, the landing distance is 1425 m. In case of a slippery runway or a steeper angle of attack, reverse thrust can be applied to secure a short landing distance.

## 4.4 Fuselage design

### 4.4.1 Fuselage design choices

**Seat configuration** The hydrogen tanks on top of the aircraft might be able to converge a little bit into the aisle. Therefore, a symmetric seat configuration with two or three seats at each side is the most convenient. Using a standard seat pitch and width, the total length and fuselage diameter can be determined. The three seat configuration would imply a slightly larger diameter but shorter fuselage. This increased diameter fits the cargo and business seats better[19]. The seat configuration is seen in Figures B.1, B.2 and B.3 and Tables 11, 12 and 13.

**Cargo** The cargo storage locations and sizes are seen in Figures B.2 and B.3 and Tables 12 and 13. The carry-on luggage is to be stored above the passengers. The storage size is 0.25m x 0.45m along the whole passenger cabin, similar to the maximum carry-on size that airlines implement [20]. Due to the 3x3 seat configuration, the outer diameter of the fuselage is 3.5 m. Using the relation between the outer and inner layer,  $D_{out} = 1.07 \cdot D_{in}$  and seat width, the aisle appears to be wide enough. Additionally, the fuselage allows the cargo room to hold twice the standard LD 2 containers [19].

**(Emergency) exits** For the exits there are many standard sizes; type B has been chosen for the airplane to ensure good accessibility, also for wheelchairs. Four exits, two at each side as seen in Figures B.1 and B.3, make sure the distance between the two exits is within the required 18.288 m by the FAA[21; 22] (see Tables 11 and 13 for the dimensions).

**Lavatories and galleys** For every fifty passengers it a lavatory is required. This means that the aircraft needs two lavatories. Standard lavatories are 0.9m x 1m and a transfer accessible lavatory 1.05 x 1.5 m for. The space that an aircraft galley requires is also dependent on the number of passengers and the range. For the aircraft a galley size of  $2.409 m^2$  is sufficient. Since there will be one bigger lavatory in the front, there is also space for a galley with the same length. To ensure that the door can still open, the width of the galley is limited to 0.75 m. In the back of the airplane is an additional galley [23; 19] to offer the required galley area (see Figures B.1 and B.3 and Tables 11 and 13 in Appendix B).

### 4.4.2 Material selection

The skin, stringers and frames will have different aluminium series. Aluminum has been chosen over composites for several reasons. Firstly it is easier to inspect in case the fuselage is damaged due to the propeller. Furthermore, shape changes of the fuselage could cause some unforeseeable damage that can be seen earlier. Secondly, aluminum is cheaper, which might encourage airlines to buy this new aircraft. The slight increase in mass, thus required fuel is a minor inconvenience. Safety is chosen over costs, but in the future other materials can be chosen. The materials chosen are Al 2024-T3 for the skin and stringers and Al 7075-T6 for the frame.

### 4.4.3 Structural analysis

The skin thickness and the spacing of both frame and stringers are determined by the loads on the fuselage. Here, aerodynamic forces are neglected, except for weight, lift and the bending stress caused by these forces and the hoop and longitudinal stress due to pressurization. In addition the fuselage is assumed to be a hollow cylinder with  $D = 3.5m$  over its whole length. The shear and moment diagrams (Figure 7) can be made using the FBD (Figure 6),  $u_{ult}$  (Section 4.2) and the weight estimation. In flight, the airplane is considered as two cantilever beams supported by the wing box quarter point, which is estimated to be at 13.9 meters from the nose [24]. In the FBD, the direction of the force is outward of the center line, e.g. a line downwards is a negative net force.

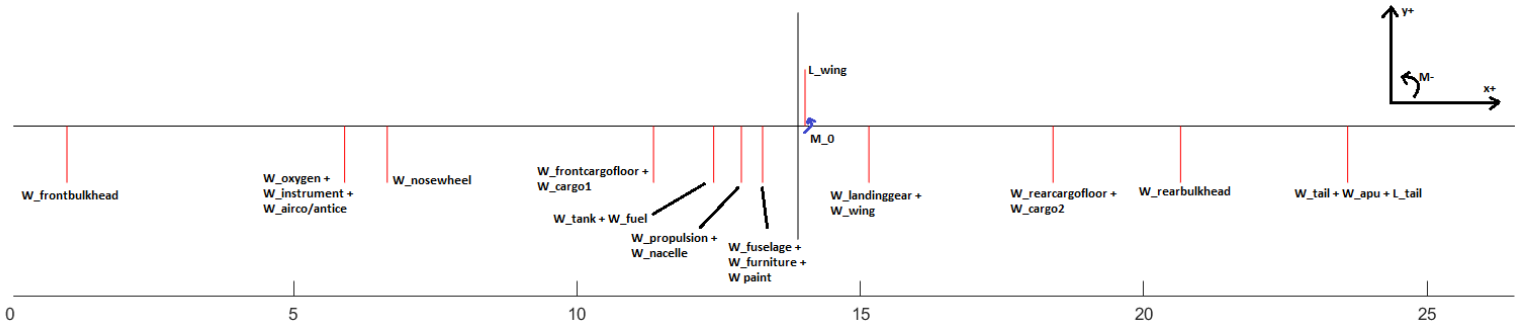


Figure 6: Free body diagram of the fuselage

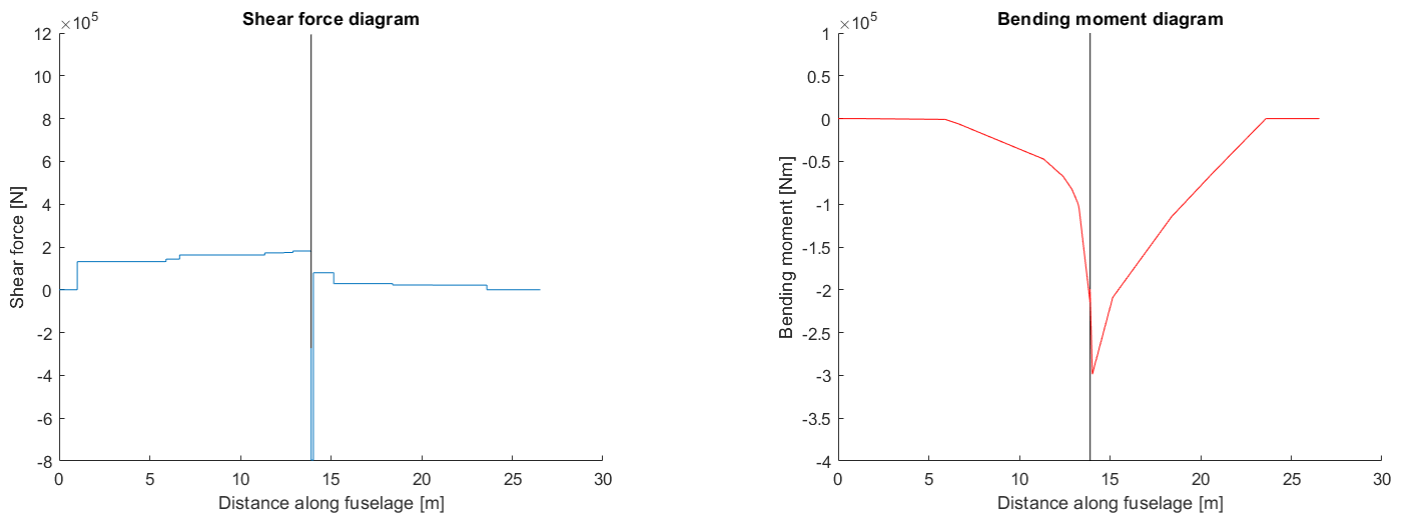


Figure 7: Shear force and bending moment diagrams

From Figure 7 the worst bending moment can be found. The skin thickness can then be determined with either Equation 10 or 11 below, depending on the highest value of the stress.

$$\frac{|M_{max}| \cdot R}{\frac{\pi \cdot ((2R)^4 - (2R-2t)^4)}{64}} + \frac{\Delta P \cdot R}{2t} = \frac{\sigma_{fatigue}}{S} \quad (10)$$

$$\frac{\Delta P \cdot R}{t} = \frac{\sigma_{fatigue}}{S} \quad (11)$$

In the this equation  $R$  is the radius of the fuselage,  $M_{max}$  is the highest bending moment,  $\Delta P$  is the pressure difference,  $S$  is the safety factor and  $\sigma_{fatigue}$  is the yield stress of the material after 30000 number of cycles. Filling in the values below gives a minimum skin thickness of  $t = 1.97$  mm.

$$R = 1.75 \text{ m} \quad M_{max} = 162196.6 \text{ Nm} \quad \Delta P = 60000 \text{ Pa} \quad \sigma_{fatigue} = 80 \text{ MPa} [25] \quad S = 1.5$$

The same values for the stress and safety factor are used for finding the space between stringers, considering the skin between two stringers as a simply supported plate with loaded edges. Solving Equation 12, then the maximum width ( $b$ ) of 0.185 m is found. This means that 60 stringers are needed over the full circumference.

$$\frac{\sigma_{fatigue}}{S} = \frac{7\pi^2 E}{12(1-\nu^2)} \left(\frac{t}{b}\right)^2 [26] \quad (12)$$

$$\frac{\sigma_{max}}{S} = \frac{P_{cr}}{A} = \frac{\pi^2 \cdot E \cdot I}{(0.5L)^2 \cdot A} [27] \quad (13)$$

Whereby the elasticity modulus ( $E$ ) of aluminum 2024 T3 is 73.1 GPa and the Poisson ratio ( $\nu$ ) is 0.33 [28]. For the shape an J stringer has been chosen, because they are useful for joining panels together.

To find the spacing between frames the critical force formula is used, this is shown in Equation 13. In this equation, the variables of of the area ( $A$ ), elasticity modulus ( $E$ ) and second moment of area ( $I$ ) are the combined values for both stringers and skin, where  $A$  and  $I$  are taken from SolidWorks. The values found are shown below together with the maximum stress occurring in the fuselage ( $\sigma_{max}$ ) and the safety factor ( $S$ ). [28]

$$\sigma_{max} = 53.333 \text{ MPa} \quad E = 73.1 \text{ GPa} \quad I = 2.682 \cdot 10^{-9} \text{ m}^4 \quad A = 4.461 \cdot 10^{-4} \text{ m}^2 \quad S = 1.5$$

Solving this equation gives the maximum spacing ( $L$ ) of 0.699 m between the frames. This means that there are 38 frames needed along the fuselage.

**Deflection** For the deflection, several boundary conditions are used. For the position at the quarter wing box  $\frac{dv}{dx}_{x=13.9} = 0$  and  $v(13.9) = 0$  are used. The second moment of area is chosen to be that of a full hollow cylinder with aforementioned thickness. The elasticity modulus is that of aluminum 2024 T3.

$$I = 0.0166 \text{ m}^4$$

$$E = 73.1 \text{ GPa}$$

The total deflection of the fuselage in the ultimate load case is found using the principle of superposition, and is shown in Figure 8.

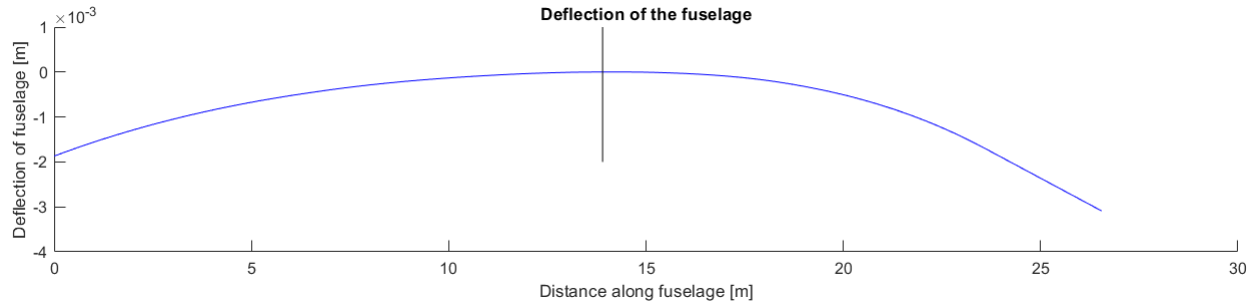


Figure 8: Deflection along the fuselage

## 4.5 Stabilizer design

The first step to designing an empennage is determining the tail moment arm, which is the distance from the aircraft's center of gravity to the aerodynamic center of the stabilizers. For an estimation, Equation 14 for the optimum tail moment arm is used.

$$l_{opt} = K_c \sqrt{\frac{4CS\bar{V}_{ht}}{\pi d_f}} \quad (14)$$

$$\bar{V}_h = \frac{l_h S_h}{C_w S_w} \quad (15)$$

$$\bar{V}_v = \frac{l_v S_v}{b_w S_w} \quad (16)$$

$K_c$  is a correction factor which is typically 1.4 for a transport aircraft.  $d_f$  is the maximum fuselage diameter, which is the outer fuselage diameter. Based on the previous Section, this value was found to be 3.5 m.  $C$  denotes the wing chord length, and  $S$  indicates the wing area (see Section 4.7). The initial values are a chord length of 3 m and a wing area of  $80.7 \text{ m}^2$ .  $\bar{V}_h$ , the horizontal tail volume coefficient, is typically 0.9 for a twin turboprop aircraft [29]. With these values plugged in,  $l_{opt} \approx 12.5$ . To determine the area of the stabilizers, Equation 15 is used for the horizontal tail, and 15 is used for the vertical tail.

As aforementioned, the horizontal tail volume coefficient  $\bar{V}_h = 0.9$  and the vertical tail volume coefficient  $\bar{V}_v = 0.08$  [29].  $l_h$  is the horizontal tail moment arm, and  $l_v$  is the vertical tail moment arm. Both values are equal to  $l_{opt}$ . Using these values in combination with the wing area, chord length, and span (see Section 4.7), the initial areas for the horizontal and vertical stabilizers are  $17.5 \text{ m}^2$  and  $14 \text{ m}^2$  respectively.

In order to obtain the lift coefficient of the horizontal stabilizer, all moments about the y-axis and the sum of forces in the z-axis are to be zero. Ignoring the pitching moments of engine thrust, wing drag, and the horizontal tail pitching moment, Equation 17 is used.

$$C_{m_{owf}} + C_L(h - h_0) - \bar{V}_{ht} C_{L_h} = 0 \quad (17) \quad C_{m_{owf}} = C_{m_{af}} \frac{AR \cos^2 \Lambda}{AR + 2 \cos \Lambda} + 0.01 \alpha_t \quad (18)$$

$h$  is the distance from the wing's aerodynamic center to the aircraft's center of gravity, which is 0.185 m for an aircraft with a full tank.  $h_0$  is the wing's aerodynamic center position, which is 0.25 of the wing chord's length.  $C_{m_{owf}}$  refers to the wing-fuselage pitching moment coefficient, which is found using Equation 18.

$C_{m_{af}}$  refers to the airfoil pitching moment coefficient, AR is the wing's aspect ratio,  $\Lambda$  is its sweep angle, and  $\alpha_t$  is the wing twist angle. Due to flight conditions, it is assumed that the latter two variables to be zero. Using the wing data, the wing-fuselage pitching moment is -0.041, and when all values are substituted in the aircraft pitching moment equation,  $C_{L_h}$  is found to be -0.36. In order to check for static longitudinal stability, Equation 19 for the change in pitching moment with respect to angle of attack is used:

$$C_{m_\alpha} = C_{L_\alpha}(h - h_0 - V_h \frac{C_{L_{\alpha_h}}}{C_{L_\alpha}} (1 - \frac{\partial \epsilon}{\partial \alpha})) \quad (19)$$

In Equation 19,  $\frac{\partial \epsilon}{\partial \alpha}$  is the downwash slope (0.01 according to wing data),  $C_{L_\alpha}$  is the wing lift slope coefficient, and  $C_{L_{\alpha_h}}$  is the horizontal tail lift slope coefficient. If the value of the equation is negative, then the aircraft is stable. The selected airfoil for the horizontal tail is NACA 0012. The corresponding angle of attack for the lift coefficient is found using Xfoil [30], and the ratio between the horizontal tail's lift coefficient and its angle of attack provides  $C_{L_{\alpha_h}}$ , which is approximately 0.121. When all the values are substituted into the static longitudinal stability equation, a value of approximately -0.197 is obtained, therefore proving that the horizontal tail provides a sufficient stability. The horizontal tail's aspect ratio is half of the wing's aspect ratio, which is 5. Its taper ratio ( $\lambda_t$ ) is assumed to be 0.5, since the typical value for tail surfaces is between 0.4 to 0.6 [31]. Other useful geometric data for the horizontal tail were found.

$$AR_t = \frac{b_t}{\bar{C}_t} \quad (20)$$

$$S = b_t \bar{C}_t \quad (21)$$

$$\lambda_t = \frac{C_{t_{tip}}}{C_{t_{root}}} \quad (22)$$

$$\bar{C}_t = \frac{2}{3} C_{t_{root}} \left( \frac{1 + \lambda_t + \lambda_t^2}{1 + \lambda_t} \right) \quad (23) \quad l_h \tan(\alpha_s - i_w - 3) < h_t < l_h \tan(\alpha_s - i_w + 3) \quad (24)$$

Equations 20 to 23 were solved simultaneously to find the horizontal tail's span ( $b_t = 9.4$  m), mean chord length ( $\bar{C}_t = 1.9$  m), tip chord length ( $C_{t_{tip}} = 1.2$  m), and root chord length ( $C_{t_{root}} = 2.4$  m). For the vertical tail, the taper ratio selected is 0.5. The typical values for the aspect ratio range from 1.2 to 1.8; a value of 1.8 has been chosen. Solving the equations, the vertical tail span is about 5 m, its mean chord length is 2.8 m, its root chord

length is 6.4 m, and its tip chord length is 3.2 m. The vertical position of the horizontal tail relative to the wing chord line is calculated using Equation 24.

$\alpha_s$  is the stall angle (15 degrees), and  $i_w$  is the wing incidence angle (1.1 degrees). This gives us a vertical height between 4.96 m and 8.31 m. The incidence angle of the wing is calculated using formula 25.

$$i_t = \alpha_h - \alpha_w + \epsilon \quad (25) \quad \epsilon = \frac{2C_{Lw}}{\pi AR} + \frac{\partial \epsilon}{\partial \alpha_w} \alpha_w \quad (26) \quad h_n = h_0 + V_h \frac{C_{L_{\alpha_h}}}{C_{L_\alpha}} \left(1 - \frac{\partial \epsilon}{\partial \alpha}\right) \quad (27)$$

$\alpha_w$  is the angle of attack of the wing (3.2 degrees),  $\alpha_h$  is the incidence angle of the tail (-2.91 according to Xfoil), and epsilon is the downwash, calculated by Equation 26. The downwash is 0.032, giving us a tail setting angle of approximately -6 degrees. The neutral point of the aircraft is calculated using Equation 27.

The neutral point is 1.67. The static margin, the difference between the neutral point and center of gravity location, is 1.47.

## 4.6 Landing gear design

### 4.6.1 Position of the landing gear

As discussed in Section 3, a retractable tricycle landing gear will be designed. For the positioning and design of the landing gear, there are two important factors to consider. The first factor is the take-off stability. During take-off, the aircraft's empennage should not hit the runway

The angle at liftoff can be estimated to be between 15° and 19°. Therefore, for the calculations, it was chosen to use 19° as a first estimation. [19]

The second major factor is the positioning of the gears concerning the centre of gravity. First of all, the centre of gravity should be between the nose gear and main gear to keep the aircraft from tipping over. This should also be the case during lift-off.

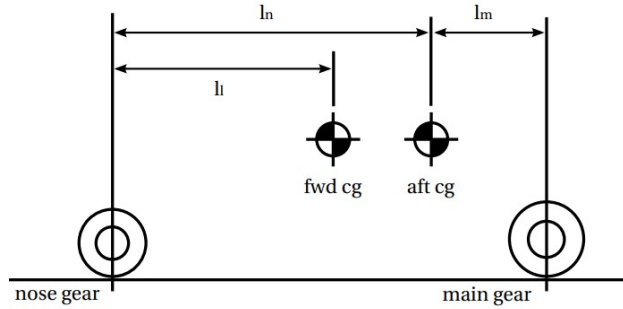


Figure 9: Dimensions of the position of the landing gear

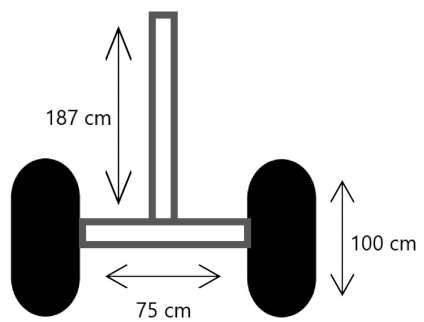


Figure 10: Simplified bogey, front view

Furthermore, it is desired to have most of the weight of the aircraft on the main gear to ensure that the braking is forceful. The maximum gear loads can be calculated using equations 28, 29 and 30 and Figure 9.

$$F_{m\ max} = \frac{l_n}{l_m + l_n} W \quad (28) \quad F_{n\ max} = \frac{l_m + l_n - l_l}{l_m + l_n} W \quad (29) \quad F_{n\ min} = \frac{l_m}{l_m + l_n} W \quad (30)$$

It has to be noted that these equations are based on today's aircraft. It is assumed that this is a valid representation of the current case. For a first estimate, a maximum and minimum nose load of 15 % and 8% respectively compared to the total weight should be chosen [6]. Together with the estimation of  $\theta_{LOF}$ , the positions of the landing gears can be calculated. Using the above equations, the optimal position for the main gear is found to be 0.378 m behind the centre of gravity and for the nose gear 4.02 m - 4.35 m in front of the centre of gravity. However, with regards to the fuselage design, an optimal position for the nose gear would be around 6.0 m in front of the centre of gravity. This can be achieved by placing the main gear 0.55 m behind the centre of gravity. The nose gear will, once retracted, be stored in the fuselage as depicted in Figure B.3. The main gears will be stored partially in the wings and partially in the fuselage.

### 4.6.2 Loads

The landing gear should be capable of carrying the whole aircraft. This means that it should be able to withstand the weight of the aircraft and the forces involved during a rough landing. As specified in the requirements, this means the gears should be able to withstand 2.1 times their maximum load. According to comparable commercial aircraft, the choice is made to have 3 bogeys in total; 1 for the nose gear and two for the main gear. Every bogey will consist of two wheels. This means that both nosewheels need to be able to take a load of at least 37983 N and the main wheels a load of at least 110935 N each. To check the feasibility of this configuration, a simplified structural analysis is performed. Figure 10 depicts a simplified bogey. The wheels are estimated to have a diameter of 100 cm. Furthermore, the beams will be estimated as hollow cylinders since multiple systems have to be present

within the structure. These cylinders have an outer diameter of 7.5 cm and an inner diameter of 6.5 cm. The maximum bending stress and shear stress in the horizontal beam can be determined by using beam analysis [32]. It was found that the maximum bending and shear stresses are 288.1 MPa and 50.28 MPa respectively. Using GRANTA Edupack [33], a list of suitable materials were found. Together with requirements stated in Section 2, the selection was further narrowed. The following material was chosen: Low alloy steel, AISI 9310, annealed. This material has a fatigue strength of about 345-518 MPa at  $10^6$  cycles, which is clearly sufficient. With the above knowledge, the critical buckling stress can be calculated. This follows that the critical buckling stress is 1.43 GPa. This clearly is sufficient for the current application. Since this is an oversimplified analysis of a landing gear, a more accurate analysis should be done during further development. However, the current analysis shows that the configuration is feasible.

## 4.7 Wing design

**General design** As already specified in section 3 our concept uses a low mounted wing in a conventional style. For stability reasons a small dihedral angle is needed. A swept wing design is only beneficial in trans to supersonic conditions. For a subsonic aircraft therefore a sweep angle of zero is chosen. The final general design choice is regarding the form of the wing. To be as close as possible to the aerodynamically favourable elliptical cord, a tapered wing is chosen. Regarding the taper ratio the findings of [34] are followed, which states that a ratio of 0.33 is optimal.

**Wingspan** Aerodynamically speaking, a long and slender wing is preferable. A limiting factor is gate accessibility. To be able to serve airports with standard III gates [35], the wingspan  $b$  is limited to a maximum of 36 meters. The fuselage with a diameter of 3.5 meters is placed between the wings. As a result, the effective aerodynamic surface can have a maximal span of 32.5 meters.

**Aspect ratio** Another important metric of a wing is its aspect ratio  $AR = \frac{b^2}{S}$ . It compares wingspan  $b$  to surface area  $S$ . Following the reasoning from the last paragraph, a high  $AR$  value indicates high efficiency. Typical modern aircraft have an  $AR$  equal to 6-8 [36]. To be at the preferable side of the spectrum, a value of at least 8 would be favored.

With these general wing requirements set in place, the following section explains the wing dimensions and the airfoil profile selection process. Moreover, the structural rigidity in maximal stress concentrations is proven.

### 4.7.1 Airfoil selection

Because the aircraft only flies in subsonic conditions, a wing with 15 percent thickness can be used. There is a large amount of predefined airfoils from multiple institutes and companies. To narrow things down, the NACA database was chosen as a starting point. Looking at the profile requirements, the series six NACA 63 - XXX definition seemed to be an appropriate option. The 6 series is not defined geometrically but instead based on aerodynamic parameters. The second digit specifies the minimal pressure location to be at the 30 percent point of the cord.

**Comparing airfoils** Using the 15 percent profile thickness mentioned before, only the third digit is undeclared yet. This parameter describes the zero alpha lift coefficient in tenths, which also reflects the camber. The two appropriate  $C_{l\alpha=0}$  magnitudes of 0.2 and 0.4 were chosen. As a result, the two airfoils being compared are the NACA 63 - 215 and NACA 63 - 415 (from now on referred to as 215 and 415), represented in Figure 11.

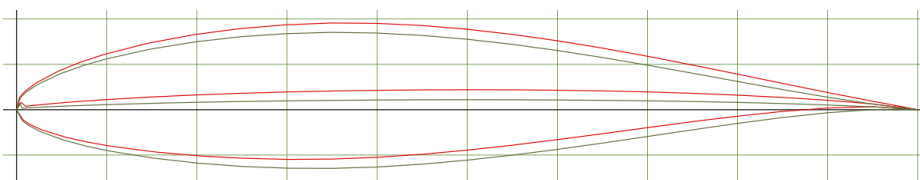


Figure 11: Airfoil profiles, 215 (green), 415 (red)

All thin airfoils'  $C_l$  curves have roughly the same linear slope in the stable alpha region. Due to the higher  $C_{l\alpha=0}$  the 415 graph is shifted to the left. This can be validated in the  $C_l$  versus  $\alpha$  graphs in Figure 12. This shift is induced by a higher camber line seen in Figure 11. Looking at the  $C_d$  graph there is no decisive difference between the two. Now plotting  $\frac{C_L}{C_D}$  versus  $\alpha$  finds  $\frac{C_L}{C_{D\max}}$  of 415 to be 20 percent higher. The absolute moment coefficient value of 415 is roughly double the magnitude of 215.

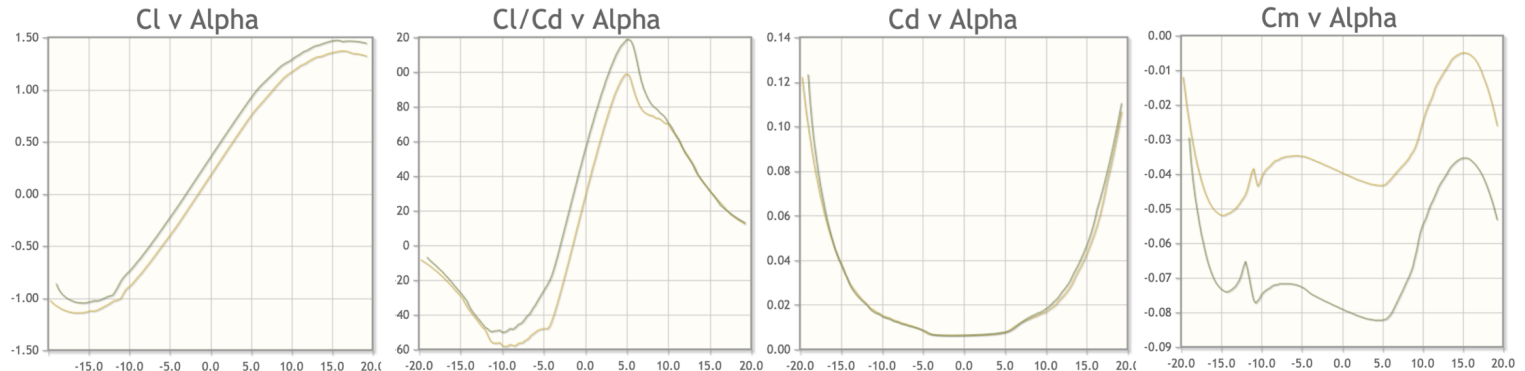


Figure 12: Airfoil coefficients, 215 (yellow), 415(green)

**NACA 63 - 215** There are only minor efficiency and performance benefits for the global aircraft, when increasing the lift to drag ratio of the wing profile in the region above 100. In addition, scaling up the pitching moment by a factor of two has a major negative effect on stability and structural properties of the aircraft. Following this reasoning the NACA 63 – 215 is chosen as the airfoil profile for the main wing of the aircraft.

**Cruise** To determine the most ideal mounting angle and dimensions of the wing, the profile is analyzed in cruise conditions. All relevant values are summarized in Table 5. To keep the required thrust minimal, the zero lift drag  $C_{D0}$  should equal  $C_{Di}$  [36]. The equation for the optimal lift coefficient can be found as 31. AR and  $C_{d0}$  are obtained from earlier iterations. The Oswald factor  $e$  is estimated with equation 32 [37]. The acquired lift coefficient can now be used in Xfoil [30] to find the effective angle of attack 13.

Table 5: Cruise condition

Property	Speed	Mass	Weight	Height	Temperature	Air density	Viscosity	Speed of sound	Reynolds	Mach
Value	152.78	24975	245000	9000	229.66	0.466	1.50E-05	303.83	4.75E+06	0.5
Dimension	$\frac{m}{s}$	kg	N	m	K	$\frac{kg}{m^3}$	$\frac{Ns}{m^2}$	$\frac{m}{s}$		

$$C_l = \sqrt{\pi e A R C_{D0}} \quad (31)$$

$$e = \frac{1}{1.05 + 0.007\pi A R} \quad (32)$$

$$\alpha_i = \frac{C_l}{\pi e A R} \quad (33)$$

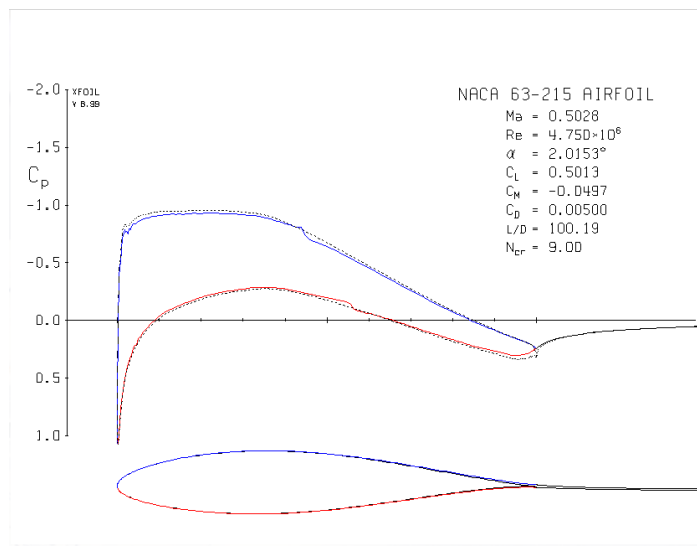


Figure 13: Airfoil in cruise conditions

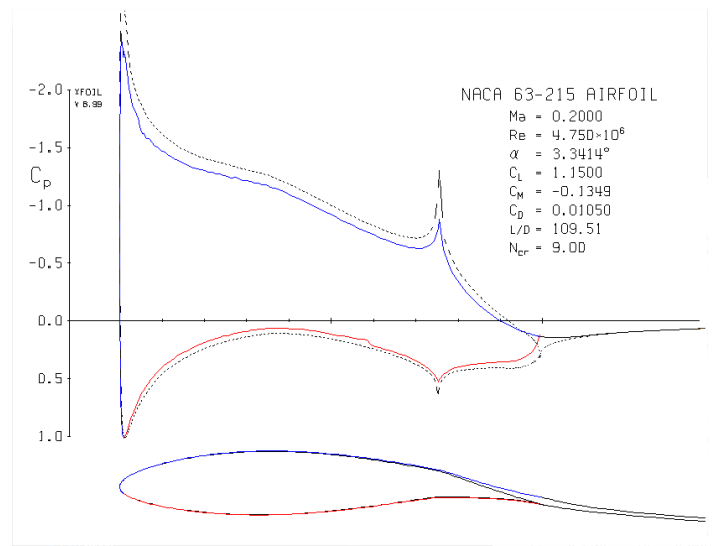


Figure 14: Airfoil with flap at 9 degree deflection

To calculate the actual mounting angle of the wing, the induced angle of attack shown in equation 33 is added to  $\alpha_{eff}$ . In cruise conditions lift has to equal the weight of the aircraft. The required wing area  $S$  can be calculated by rearranging the standard lift formula 34. The missing dimensions of the wing can now be easily derived with the taper ratio  $t$  and aspect ratio  $AR$  (see equations 35, 36, 37 and 38). All numerical values for angles and dimensions are summarized in Table 6.

$$S = \frac{2W}{\rho C_l V^2} \quad (34)$$

$$b = \sqrt{A R S} \quad (35)$$

$$c_{mean} = \frac{S}{b} \quad (36)$$

$$c_{root} = \frac{2}{(1+t)c_{mean}} \quad (37)$$

$$c_{tip} = \frac{2}{(1-t)c_{mean}} \quad (38)$$

Table 6: Wing dimensions

Variable	$\alpha_{eff}$	$\alpha_i$	$\alpha_{mount}$	A	b	$c_{mean}$	$c_{tip}$	$c_{root}$	max. $h_{tip}$	max. $h_{root}$
Value	2.01	1.15	3.17	90.41	30.07	3.00	1.49	4.52	0.22	0.68
Dimension	degree	degree	degree	$m^2$	m	m	m	m	m	

**Landing and Take off** Now that all dimensions are set, the special requirements in landing and takeoff are analyzed. Using the take-off requirements set by the engine design,  $C_l = 1.15$  has to be achieved. To be able to do this high lift devices are needed. After iterating over different options a plain flap was found to be sufficient. This simple flap increases camber without changing wing area, by deflecting the trailing edge downwards. The flap hinge is placed at three quarters cord length to the leading edge. Investigating the design in Xfoil [30] (see Figure 14) gives a deflection angle of 9 degrees. With the fixed mounting angle (See Table 6) at take-off, the profile can now produce the required  $C_l$ . The flap setup is also used to reach the required  $C_l$  during landing. Moreover, to decrease the distance after touch down even further, spoilers are installed. When deployed, they eliminate the lift and increase drag dramatically.

#### 4.7.2 Stress calculation

The loads on the wing can be separated into point and distributed forces. The weight of the engine  $E$  is represented as a point force placed at distance  $e$  from the root. All aerodynamic forces and moments are estimated to be constantly distributed over the span of the wing. The total maximal lift can be derived with the maximal load factor taken from Figure 1 described in [15] and the weight of the aircraft[15]. Drag and moment values are found by using the standard formulas analyzed at highest flight speeds. For the weight of the wings, the estimation from Table 4 can be used. The distributed magnitudes can be calculated by dividing the absolute force or moment by the length of the wing. Beside the free body diagram in Figure 15, all magnitudes can be found in Table 7.

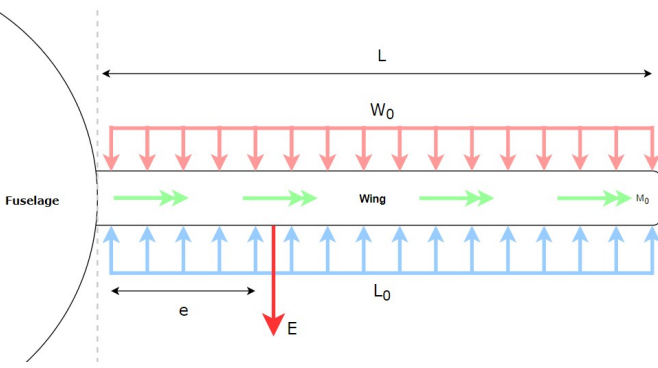


Figure 15: Free body diagram wing

Table 7: Magnitudes of Figure 15

Variable	Value	Dimension
L	15	m
e	2.7	m
$M_0$	4899	Nm/m
$W_0$	120	N/m
$L_0$	39710	N/m
$D_0$	533	N/m
E	7063	N

**Spar** A box design combines excellent torsional behavior of a closed profile, with high bending inertia at a low weight. Therefore, the decision was made to settle for the box form factor.

Analyzing the free body diagram of Figure 15 with the standard beam theories [38] lead to the following force and moment graphs in Figure 16.

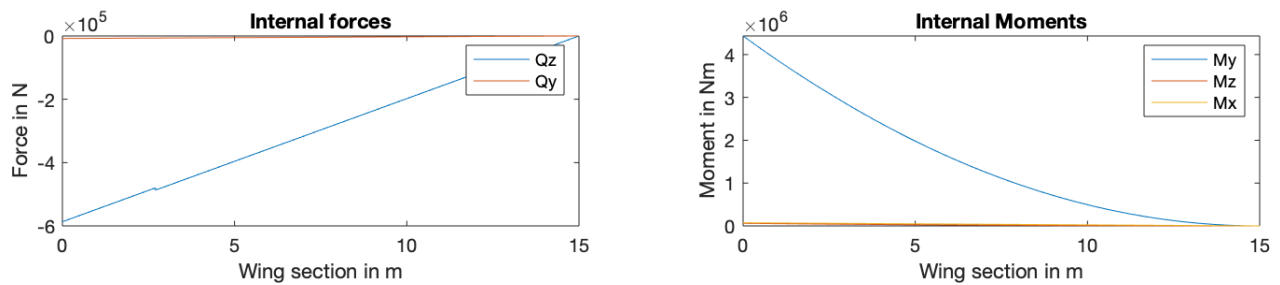


Figure 16: Maximal internal forces and moments across the wing

For the stress, the spar is assumed as a hollow rectangle with wall thickness  $t = 2cm$ . Identical to the wing, the spar is also modeled in a tapered manner with root height  $H = 0.67m$  and width  $B = 1.00m$ . The maximal stress is set by the Swain equation (Equation 39)[38]. The bending moment of inertia for a hollow rectangle can be calculated as in Equation 40.

$$\sigma_{max} = \frac{M_y(x)}{I_y(x)} z_{max} + \frac{M_z(x)}{I_z(x)} y_{max} \quad (39)$$

$$\tau_{max} = \frac{M_x(x)}{2A_m(x)t} \quad (41)$$

$$I(x) = \frac{BH^3 - (B - 2t)(H - 2t)^3}{12} \quad (40)$$

The values are dependent on  $x$ , the location along the wing. Now plotting the maximal stress in Figure 17 on each location, proofs that the maximal bending stress occurs at the root of the wing at about 240 MPa. For the maximal torsional shear stress, Bredt's formula [38] in Equation 41 is used. Similar to bending the maximal torsional shear stress is plotted for each  $x$ -location in Figure 17. With a maximum of 10 MPa around the midpoint of the wing, the stress is quite low. As a result, the torsional deflection will be minimal, which will in turn prevent negative effects like divergence and flutter. For the spar material, a carbon fiber composite is selected. Due to the tapered and hollow shape of the wing box, manufacturing the whole spar as one part is impossible with a metal alloy. Fiber composites can already be woven in a tube-like form factor. With strengths of 790 MPa [39], an extremely light and stiff spar can be manufactured.

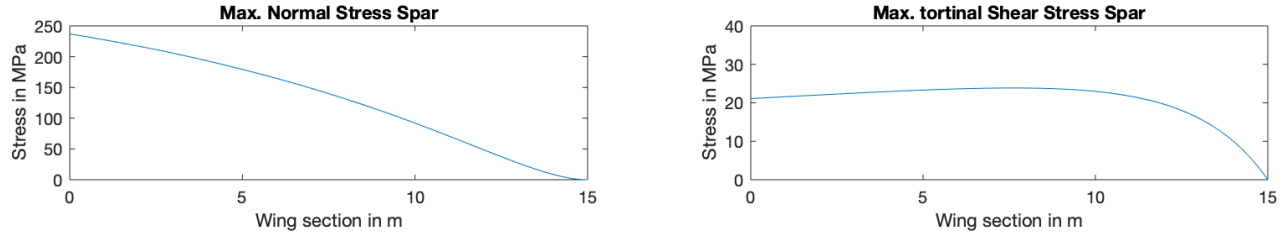


Figure 17: Maximal bending and torsional stress across wing

**Ribs and stringers** To estimate rib distance and stringer placement, buckling theories were used [27; 26]. Global buckling estimates the wings' skin and stringers as a beam. The stringers are represented as rectangles with measures 8 cm x 2 cm each. The global buckling equation (Equation 42) is rearranged for the critical rib distance  $l_{cr}$  as seen in Equation 43.

$$F_{cr} = \frac{\pi^2 EI}{l_{eff}^2} \quad (42) \quad l_{cr} = \sqrt{\frac{\pi^2 EI}{F_{max}}} \quad (43) \quad F_{max} = \sigma_{mx} A \quad (44) \quad \sigma_{cr} = \frac{k\pi^2 E}{12(1-v^2)} \left(\frac{t}{b}\right)^2 \quad (45)$$

The resulting plot in Figure 18 shows that close to the root the critical rib distance is minimal. This means that ribs have to be placed closer together near the root compared to the tip of the wing. The suggested rib placement across the wing is indicated as red lines in Figure 18. In total nine ribs are installed.

In local buckling, each skin panel between the ribs and stringers is evaluated. The critical stress in Equation 45 on plate buckling is compared to the actual stress in maximal load conditions. As long as the actual curve is below the critical limit, no buckling will occur. Factor  $k$  can be found in [26]. Panel width can be calculated through dividing the cord length by the number of stringers.

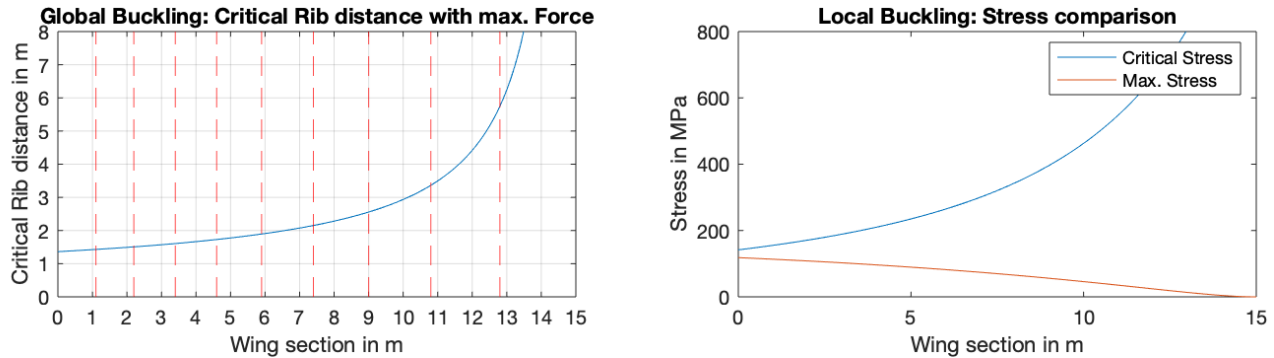


Figure 18: Global and local buckling

Iterating over different materials, a total of 12 stringers and a skin thickness of 2 mm was chosen. Due to compression and tension stress two aluminum alloys were selected. To resist buckling the upper surface of the wing is made of the extremely strong 7075 T6 series. The 2024 T3 alloy is used for the tensioned lower skin. Although the material is not as strong, the fatigue behavior in aircraft use cycles is much better.

**Deflection** Similar to the fuselage, the wing's total deflection is found. The principle of superposition is used to sum the deflections by the forces. The total deflection of one wing can be found in Figure 19 for two different load cases.

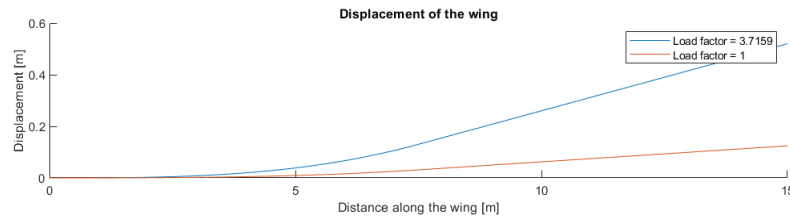


Figure 19: Deflection of the wing

## 4.8 Engine Design

### 4.8.1 Required Power

In Figure 4 it can be seen that most power is required during take off and at velocities higher than the cruising velocity. Therefore, the required engine power is based on the desired runway length. The thrust required to take off can be calculated with Equation 46.

$$T_{LO} = \frac{1.44W^2}{g\rho SC_{L,max}s_{LO}} + [D_{tot} + \mu_{LO}(W - L)]0.7V_{LO} \quad (46)$$

$$P_{engine,LO} = \frac{T_{LO}V_{LO}}{\eta} \quad (47)$$

In order to calculate the power the engine has to provide during take-off, the thrust has to be multiplied by the take off velocity (Equation 7), and divided by the propeller efficiency, as shown in Equation 47.

The values for the different variables used in Equation 46 and 47 are given in Table 8.

Variable	W	$\rho$	S	$C_{L,max}$	$C_{D,0}$	$s_{LO}$	e	AR	h	b	$\mu_{LO}$	$\eta$
Magnitude	239688	1.225	89.8	1.15	0.01973	1500	0.8	10	2	26.8	0.02	0.75
Units	N	$kg/m^3$	$m^2$	-	-	m	-	-	m	m	-	-

Table 8: Magnitudes of variables used to calculate the liftoff power

In this table, all variables are a function of the shape, size and content of the aircraft, except the rolling friction coefficient,  $\mu_{LO}$ . This is taken to be 0.02 for asphalt [17], which will be material from which the aircraft will take off. The average propeller efficiency  $\eta$  during liftoff is estimated to be 0.75 [40]. With these values taken into consideration, the required power for liftoff is 5.4 MW. However, if the aircraft faces an unforeseen tailwind, asphalt that is slightly more rough, or some other factor, which makes taking off with the power available impossible, it is necessary to have some power. Therefore this minimum amount of power is multiplied with a safety factor of 1.15, which makes the required engine power 6.24 MW.

### 4.8.2 Engine Size and Weight

When scaled in comparison to engines in the same power range, the engines will weigh approximately 602 kg each, have a height of 112 cm, a width of 72 cm and a length of 226 cm [41] [42].

### 4.8.3 Power system efficiency

The energy to transport the aircraft from one airport to the other is initially stored chemically in the hydrogen bonds. In order to convert this to kinetic and gravitational energy, the hydrogen is burned in the turbine engine's combustion chamber. It is assumed that the chemical efficiency of a turboprop engine is 50%, the gearbox efficiency is 98%, and the propeller efficiency varies from 75% on average during take off, to 80% during cruise [43].

### 4.8.4 Propeller

**Number of propeller blades** Since this concept has a low wing configuration, a relatively high landing gear is required in order to prevent the propeller blades from hitting the ground. In order to limit the weight and size of this landing gear, the propeller size should be limited. From an efficiency point of view, it is better to have as little propeller blades as possible. However, in order to deliver the thrust generated by the engine to the air, the propellers would have to be relatively long. In order to reduce the required propeller diameter, more propeller blades can be used. Therefore it is chosen to have 6 propeller blades to reduce the required propeller diameter. Entire propeller systems of this type are available at Collins Aerospace, and include pitch control and heating in the propeller blades to prevent ice forming. Aircraft comparable in size and performance to this concept (such as the ATR 72, Bombardier Aerospace Q400 and Ilyushin il-114) also use six bladed propeller systems.

**Diameter** The desired propeller diameter can be obtained from a combination of two approaches. Firstly, the propeller diameter can be approximated by a statistical approach. Secondly, the propeller should be as large as possible, without the propeller tips entering the transonic regime. The smallest of the two obtained values is picked for the initial layout [3].

The propeller diameter can be determined statistically based on Equation 48 [3]:

$$D = K_p \sqrt[4]{Power} = 0.49 \sqrt[4]{\frac{6240}{2}} = 3.66m \quad (48)$$

$$V_{tip,helical} = \sqrt{V_\infty^2 + (r\omega)^2} \quad (49)$$

In the case of the propeller having four or more blades, the value for  $K_p$  is 0.49. In the equation, the power is expressed in kW. When the values are filled in (Equation 48), a diameter of 3.66 m is obtained.

In order to check whether the propeller tips do not move too fast, the helical velocity of the propeller has to be calculated. As the aircraft moves through the air, the propellers make a helical path through the air. This helical

velocity is the vector sum of the free stream velocity approaching the aircraft ( $V_\infty$ ) and rotational velocity of the propeller ( $r\omega$ ). This means that maximum helical tip velocity can be calculated with Equation 49.

A typical engine with a peak power of  $3.4 \text{ MW}$ , such as the Pratt & Whitney P150, has a maximum output shaft velocity of  $1020 \text{ rpm}$  [41]. The cruise velocity is calculated to be  $152.7 \text{ m/s}$  (Equation 7). So in case the propeller is spinning at its maximum rotational velocity during cruise (which will be a worst case scenario), the helical tip velocity will be  $248 \text{ m/s}$  or Mach  $0.72$ , which is acceptable [3].

#### 4.8.5 Engine placement

The minimum clearance from the blade tips to the fuselage can be calculated by having  $10 \text{ cm}$  added to  $1.65 \text{ cm}$  per every  $75 \text{ kW}$  of engine power [44]. For an engine of  $3.35 \text{ MW}$  this reduces to  $85 \text{ cm}$ . Placing the engines further outward on the wing will reduce the noise experienced in the cabin. However, in case of a single engine failure, this would also require larger control surfaces on the tail. Therefore it is chosen to place the engines as close to the fuselage as possible, with the center of the propellers at  $85 + 183 = 268 \text{ cm}$  from the fuselage.

## 5 Evaluation and Conclusion

In Section 2, the requirements for the aircraft were discussed. The most relevant requirements took the safety and functionality of the aircraft into account. The airplane has to cruise at an altitude of  $9000 \text{ m}$  with a velocity of  $550 \text{ km/h}$ . In these conditions, it has to be able to reach destinations in a range of  $800$  to  $1000 \text{ km}$ , while carrying at least  $80$  passengers of  $90 \text{ kg}$  each, with an additional  $20 \text{ kg}$  of luggage. The aircraft and its materials are designed based on these cruising requirements and circumstances. Also, it should take-off and land on a  $1500\text{m}$  runway, to be employable as a regional airliner. This requirement to take-off is met, since the necessary runway length is  $1260 \text{ m}$  and  $1425 \text{ m}$  for take-off and landing respectively. The aircraft concept was also based on the requirements with respect to the size restrictions, for example, set by the airports where the aircraft possibly lands. With a span  $b = 33.5 \text{ m}$ , it will fit at most gates. During the calculations, safety factors and regulations were taken into account and were met; for example the emergency exits. Most importantly, the aircraft will fly on hydrogen, such that it will not release any green-house gases in-flight. Generally speaking, this aircraft is similar to existing aircraft. This is to make sure the design is (financially) attractive for manufacturers and airlines. This choice makes the aircraft safer as well, since most of its elements and materials are in use and a lot of knowledge is gained already.

# Bibliography

- [1] D. Silberhorn, G. Atanasov, J.-N. Walther, and T. Zill, "Assessment of hydrogen fuel tank integration at aircraft level," 09 2019.
- [2] D. Raymer, "Aircraft design: A conceptual approach," AIAA education series, ch. 10.2, American Institute of Aeronautics and Astronautics, Incorporated, 2018.
- [3] D. Raymer, "Aircraft design: A conceptual approach," AIAA education series, ch. 10.4, American Institute of Aeronautics and Astronautics, Incorporated, 2018.
- [4] N. Van Zon, "Liquid Hydrogen Powered Commercial Aircraft," 2018.
- [5] Tronair, "TYPES OF LANDING GEAR EQUIPMENT AND AIRCRAFT SERVICING TOOLS." <https://www.tronair.com/resources/types-of-landing-gear-equipment-and-aircraft-servicing-tools#:~:text=Landing%20gear%20usually%20comes%20in,inside%20an%20aircraft%20during%20flight..>, 2020. Website accessed on 14-12-2020.
- [6] N. Heerens, "Landing gear design in an automated design environment," 2014.
- [7] J. Roskamp, "Airplane Design, Part IV: Layout Design of Landing Gear and Systems." <https://www.librarything.com/work/2656500>, 2020. Website accessed on 14-12-2020.
- [8] L. Stein, "Would you travel on a windowless plane? emirates is looking to use virtual ones instead?" <https://www.abc.net.au/news/2018-06-07/would-you-travel-on-a-windowless-plane/9843722>, 2021. Website accessed on 09-01-2021.
- [9] "The windowless plane." <https://www.uk-cpi.com/windowless-plane>, 2021. Website accessed on 03-01-2021.
- [10] O. Al-Shamma and R. Ali, "Aircraft weight estimation in interactive design process." [https://uhra.herts.ac.uk/bitstream/handle/2299/10741/Aircraft\\_weight\\_estimation\\_in\\_interactive\\_design\\_process.pdf?sequence=2](https://uhra.herts.ac.uk/bitstream/handle/2299/10741/Aircraft_weight_estimation_in_interactive_design_process.pdf?sequence=2), 2021.
- [11] I. Sen, "Aircraft fuselage design study." Download item, 2021. Website accessed on 11-01-2021.
- [12] F. A. Administration, "Part 23 AIRWORTHINESS STANDARDS: NORMAL, UTILITY, ACROBATIC, AND COMMUTER CATEGORY AIRPLANES." [https://rgl.faa.gov/Regulatory\\_and\\_Guidance\\_Library%5CrgFAR.nsf/0/D35E170180C8CB2185256687006D0C90?OpenDocument](https://rgl.faa.gov/Regulatory_and_Guidance_Library%5CrgFAR.nsf/0/D35E170180C8CB2185256687006D0C90?OpenDocument), 2020. Website accessed on 03-01-2020.
- [13] D. Scholz, "Mass and center of gravity." <https://www.fzt.haw-hamburg.de/pers/Scholz/H00U/>, 2020. Last updated on 05-04-2020.
- [14] U. D. of Transportation and F. A. Administration, "Advisory circular design dive speed," 10 1997.
- [15] T. H. G. Megson, *Aircraft Structure for Engineering Students*. 6 ed., 2017.
- [16] R. Isacco, "Design guidelines for gust load inclusion in aeroelastic optimization of a civil aircraft in the preliminary design phase," 2019.
- [17] J. D. Anderson Jr, "Introduction to flight," ch. 6, McGraw-Hill Education, New-York, 8 ed., 2016.
- [18] M. Zhang, Q. Huang, S. Liu, and H. Li, "Assessment method of fuel consumption and emissions of aircraft during taxiing on airport surface under given meteorological conditions," *Sustainability*, vol. 11(21), pp. 1–21, Nov. 2019.
- [19] "Fuselage design." [https://www.fzt.haw-hamburg.de/pers/Scholz/H00U/AircraftDesign\\_6\\_Fuselage.pdf](https://www.fzt.haw-hamburg.de/pers/Scholz/H00U/AircraftDesign_6_Fuselage.pdf), 2020. Website accessed on 11-12-2020.
- [20] "Airline Carry On Luggage Size and Weight Restrictions: A Detailed Guide." <https://www.neverendingvoyage.com/how-to-travel-carry-on-only-airline-size-and-weight-guide/#:~:text=The%20most%20commonly%20allowed%20airline,you%20plan%20to%20travel%20with>, 2020. Website accessed on 11-12-2020.
- [21] FAA, "Uniform distribution of exits." [https://www.faa.gov/documentLibrary/media/Advisory\\_Circular/AC\\_25\\_807-1.pdf](https://www.faa.gov/documentLibrary/media/Advisory_Circular/AC_25_807-1.pdf), 2020. Website accessed on 11-12-2020.
- [22] "Sec. 25.807 — Emergency exits.." <https://www.risingup.com/fars/info/part25-807-FAR.shtml>, 2020. Website accessed on 11-12-2020.
- [23] "Aircraft Lavatory Accessibility." [https://www.transportation.gov/sites/dot.gov/files/docs/3a.P4.Lav\\_.OEM\\_.Airline%20Accessible%20Lav.Position.8.15.16..pdf](https://www.transportation.gov/sites/dot.gov/files/docs/3a.P4.Lav_.OEM_.Airline%20Accessible%20Lav.Position.8.15.16..pdf), 2020. Website accessed on 11-12-2020.
- [24] J. Lusk, "Wing and Fuselage Structural Optimization Considering Alternative Material Systems." [https://kuscholarworks.ku.edu/bitstream/handle/1808/4015/umi-ku-2556\\_1.pdf;jsessionid=9C6C7A28734EF76C665EE9F6CA1FEDE4?sequence=1](https://kuscholarworks.ku.edu/bitstream/handle/1808/4015/umi-ku-2556_1.pdf;jsessionid=9C6C7A28734EF76C665EE9F6CA1FEDE4?sequence=1), 2020. Website accessed on 04-01-2021.
- [25] T. Bor, "Aircraft structures, materials in aerospace: fatigue," 2021. Accessed on 12-01-2021.
- [26] W. Grouve, "Aircraft structures, local buckling," 2021. Accessed on 12-01-2021.

- [27] W. Grouve, “Aircraft structures, global buckling,” 2021. Accessed on 12-01-2021.
- [28] L. MatWeb, “Aluminum 2024-T3.” <http://www.matweb.com/search/DataSheet.aspx?MatGUID=57483b4d782940faaf12964a1821fb61&ckck=1>, 2020. Website accessed on 04-01-2021.
- [29] M. Sadraey, “Chapter 6 Tail Design.” [http://www.aero.us.es/adesign/Slides/Extra/Stability/Design\\_Tail/Chapter%206.%20Tail%20Design.pdf](http://www.aero.us.es/adesign/Slides/Extra/Stability/Design_Tail/Chapter%206.%20Tail%20Design.pdf), 2020. Website accessed on 2-12-2020.
- [30] “Xfoil6.99.” <http://web.mit.edu/drela/Public/web/xfoil/>, 2020.
- [31] “Tail Design.” <http://aerodesign.stanford.edu/aircraftdesign/stability/taildesign.html>, 2020. Website accessed on 30-12-2020.
- [32] R. Hibbeler, *Statics and Mechanics of Materials*. 3 ed., 2011.
- [33] “Granta edupack 2020.” <https://www.ansys.com/products/materials/granta-edupack>, 2020.
- [34] T. Chen and J. Katz, “Induced drag of high-aspect ratio wings,” 01 2004.
- [35] K. C. Bishop and R. J. Hansman, “Assessment of the ability of existing airport gate infrastructure to accommodate transport category aircraft with increased wingspan for improved fuel efficiency.” <https://core.ac.uk/download/pdf/4435263.pdf>, 2021. Website accessed on 11-01-2021.
- [36] J. D. Anderson Jr, “Introduction to flight,” ch. 9, McGraw-Hill Education, New-York, 6 ed., 2016.
- [37] D. Scholz, “Estimating the oswald factor from basic aircraft geometries.” [https://www.fzt.haw-hamburg.de/pers/Scholz/OPerA/OPerA\\_PUB\\_DLRK\\_12-09-10.pdf](https://www.fzt.haw-hamburg.de/pers/Scholz/OPerA/OPerA_PUB_DLRK_12-09-10.pdf), 2021. Website accessed on 11-01-2021.
- [38] D. Gross, W. Hauger, and W. Schnell, *Technische Mechanik: Band 2: Elastostatik*. Springer-Lehrbuch, Springer Berlin Heidelberg, 2013.
- [39] S. Feih and A. Mouritz, “Tensile properties of carbon fibres and carbon fibre–polymer composites in fire,” *Composites Part A-applied Science and Manufacturing - COMPOS PART A-APPL SCI MANUF*, vol. 43, 05 2012.
- [40] D. Raymer, “Aircraft design: A conceptual approach,” AIAA education series, ch. 13.8, American Institute of Aeronautics and Astronautics, Incorporated, 2018.
- [41] Pratt and Whitney, “PW100/PW150, the power behind regional airline turboprops.” <https://www.pwc.ca/PW100-150>, 2020. Website accessed on 23-11-2020.
- [42] various, “Turboprop.” <https://en.wikipedia.org/wiki/Turboprop>, 2021. Website accessed on 08-01-2021.
- [43] M. Hepperle, “Electric flight - potential and limitations,” Oct. 2012.
- [44] E. torenbeek, “Synthesis of subsonic airplane design: An introduction to the preliminary design of subsonic general aviation and transport aircraft, with emphasis on layout, aerodynamic design, propulsion and performance,” ch. 6, Delft University Press, Delft, 1982.
- [45] IATA, “IATA - IATA Forecast Predicts 8.2 billion Air Travelers in 2037.” <https://www.iata.org/en/pressroom/pr/2018-10-24-02/>, 2020. Website accessed on 25-11-2020.
- [46] P. Campbell, “Profitability margins per industry.” <https://financialrhythm.com/profitability-margins-industry/>, 2020. Website accessed on 25-11-2020.
- [47] R. Thomson, “AIRCRAFT ELECTRICAL PROPULSION.” <https://www.rolandberger.com/en/Insights/Global-Topics/Electric-Propulsion/>, 2020. Website accessed on 25-11-2020.
- [48] Plane, “Charting the decline in air traffic caused by COVID-19,” 2020.
- [49] WorldBank, “Air transport, passengers carried | data.” [https://data.worldbank.org/indicator/IS.AIR.PSGR?end=2018&most\\_recent\\_value\\_desc=false&start=2018&view=map](https://data.worldbank.org/indicator/IS.AIR.PSGR?end=2018&most_recent_value_desc=false&start=2018&view=map), 2020. Website accessed on 25-11-2020.
- [50] WDI, “The world by income and region.” <https://datatopics.worldbank.org/world-development-indicators/the-world-by-income-and-region.html>, 2020. Website accessed on 25-11-2020.
- [51] CarbonBrief, “Global survey: Where in the world is most and least aware of climate change? | carbon brief.” <https://www.carbonbrief.org/global-survey-where-in-the-world-is-most-and-least-aware-of-climate-change>, 2020. Website accessed on 25-11-2020.
- [52] T. M. Lee, E. M. Markowitz, P. D. Howe, C. Y. Ko, and A. A. Leiserowitz, “Predictors of public climate change awareness and risk perception around the world,” *Nature Climate Change*, vol. 5, pp. 1014–1020, nov 2015.
- [53] A. M. Mccright and R. E. Dunlap, “The Politicization Of Climate Change And Polarization In The American Public’s Views Of Global Warming, 2001-2010,” *Sociological Quarterly*, vol. 52, pp. 155–194, mar 2011.

- [54] WorldBank, “New country classifications by income level: 2019-2020.” <https://blogs.worldbank.org/opendata/new-country-classifications-income-level-2019-2020>, 2020. Website accessed on 25-11-2020.
- [55] UniversityOfTwente, “Project description,” 2021.
- [56] Airbus, “Decarbonisation, towards more sustainable air travel for future generations.” <https://www.airbus.com/company/sustainability/environment/decarbonisation.html>, 2020. Website accessed on 23-11-2020.
- [57] Boeing, “Sustainability.” <http://www.boeing.com/principles/sustainability/index.page>, 2020. Website accessed on 20-11-2020.
- [58] D. Sigler, “Loganair to pioneer island-hopping electric flight.” <http://sustainableskies.org/loganair-pioneer-island-hopping-electric-flight/>, 2020. Website accessed on 20-11-2020.
- [59] Ryanair, “Monthly CO2 reports.” [https://corporate.ryanair.com/environment/monthly-co2-report/#:\\$\sim\\$text=Ryanair%20is%20Europe's%20greenest%2Fcleanest,other%20flag%20carrier%20European%20airlines.](https://corporate.ryanair.com/environment/monthly-co2-report/#:$\sim$text=Ryanair%20is%20Europe's%20greenest%2Fcleanest,other%20flag%20carrier%20European%20airlines.), 2020. Website accessed on 23-11-2020.
- [60] C. Airlines, “Eco action.” <https://calec.china-airlines.com/csr/en/environment/action-flight.html>, 2020. Website accessed on 20-11-2020.
- [61] Y. Finance, “Southwest Airlines Co. (LUV) Income statement.” <https://finance.yahoo.com/quote/luv/financials/>, 2020. Website accessed on 10-12-2020.
- [62] T. wall street journal, “KLM Royal Dutch Airlines Income statement.” <https://www.wsj.com/market-data/quotes/KLMR/financials/annual/income-statement>, 2020. Website accessed on 10-12-2020.
- [63] “How Much of Airlines’ Revenue Comes From Business Travelers?.” <https://www.investopedia.com/ask/answers/041315/how-much-revenue-airline-industry-comes-business-travelers-compared-leisure-t.asp#:~:text=Airlines%20receive%20only%20about%2060,hotels%20and%20car%20rental%20agencies>, 2020. Website accessed on 10-12-2020.
- [64] “KLM carries record number of passengers in 2019.” <https://news.klm.com/klm-carries-record-number-of-passengers-in-2019/#:~:text=KLM%20welcomed%20a%20record%20number,2.7%25%20in%20comparison%20with%202018.>, 2020. Website accessed on 10-12-2020.
- [65] “McDonnell Douglas MD-90 Aircraft.” [https://en.wikipedia.org/wiki/McDonnell\\_Douglas\\_MD-90](https://en.wikipedia.org/wiki/McDonnell_Douglas_MD-90), 2020. Website accessed on 12-12-2020.
- [66] “Boeing 747-8 design times.” [https://en.wikipedia.org/wiki/Boeing\\_747-8](https://en.wikipedia.org/wiki/Boeing_747-8), 2020. Website accessed on 12-12-2020.

# A Requirements

Table 9: User requirements

	Criteria	Score
A.	The airplane must be able to transport at least [80 passengers] of [90 kg] with [20kg] of luggage over a distance of at least [800 km] including lift off and landing, starting with a full ‘tank’.	2
B.	The airplane must not emit any greenhouse gases once in operation, excluding NO <sub>2</sub> due to direct combustion of hydrogen and water vapor.	1
C.	The airplane must be able to reach a cruise velocity of [550 km/h] at minimum.	4
D.	The airplane must be able to reach a cruise altitude of [9000 m] at minimum.	3
E.	The airplane should be able to handle [7.5 °] ascent and descent angle with at most [5% extra runway length compared to 4.0 °]	2
F.	The cabin pressure should remain lower than the atmospheric pressure at 1800 meters. In other words, the cabin pressure may not exceed [81489.22 Pa].	1
G.	The average turnaround time, with full ground service, should be [30 minutes] or less.	4
H.	The airplane must be able to withstand temperatures from [-50°C to 45°C] and pressures differences up to [60000 Pa].	2
I.	The airplane should be able to use at least [50%] of the available gates at an average airport.	3
J.	The design life of the airplane should be at least 40000 flight hours, in addition it should be able to land and lift-off at least [60000 times].	5
K.	The airplane should not contain materials that might be a hazard for people, animals and the environment once crashed.	1
L.	Passengers should be able to have a view of the outsides of the airplane.	1
M.	Diversion capabilities of [10%] of the range and [10%] of the flying time (headwind).	3
N.	The airplane should be recyclable for [80%] after service.	3
O.	The airplane should be able to land at a runway of [1500 meter] at maximum.	3
P.	During landing, the peak recorded vertical acceleration should not exceed [2.1G] or the limit load on the airframe or landing gear.	2
Q.	The aircraft should be able to operate continuously for a period of at least [36 hours] without other servicing than replacing the battery pack or loading fuel and performing a pre-flight check. Maintenance after this period should not take longer than [2 hours].	3

Table 10: Requirement rating

	A	B	C	D	E	F	G	H	I	J	K	L	M	N	O	P	Q
A	X	B	A	A	A	F	A	H	A	A	K	A	A	A	A	P	Q
B	-	X	B	B	B	F	B	H	B	B	K	B	B	B	B	P	B
C	-	-	X	D	C	F	C	H	C	J	K	C	C	C	C	P	Q
D	-	-	-	X	D	F	D	H	D	J	K	D	D	D	D	P	Q
E	-	-	-	-	X	F	E	H	E	J	K	E	E	E	E	P	Q
F	-	-	-	-	-	X	F	F	F	F	F	F	F	F	F	F	F
G	-	-	-	-	-	-	X	H	G	J	K	G	M	G	G	P	Q
H	-	-	-	-	-	-	-	X	H	H	H	H	H	H	H	P	H
I	-	-	-	-	-	-	-	-	X	J	K	I	M	N	O	P	Q
J	-	-	-	-	-	-	-	-	-	X	K	J	J	J	J	P	Q
K	-	-	-	-	-	-	-	-	-	-	X	K	K	K	K	P	K
L	-	-	-	-	-	-	-	-	-	-	-	X	M	N	O	P	Q
M	-	-	-	-	-	-	-	-	-	-	-	-	X	M	M	P	Q
N	-	-	-	-	-	-	-	-	-	-	-	-	-	X	O	P	Q
O	-	-	-	-	-	-	-	-	-	-	-	-	-	-	X	P	Q
P	-	-	-	-	-	-	-	-	-	-	-	-	-	-	-	X	P
																	X
	1	2	3	4	5	6	7	8	9	10	11	12	13	14	15	16	17
	F	P	H	K	B	Q	A	J	D	C	E	M	G	O	N	I	L

## B Fuselage drawings

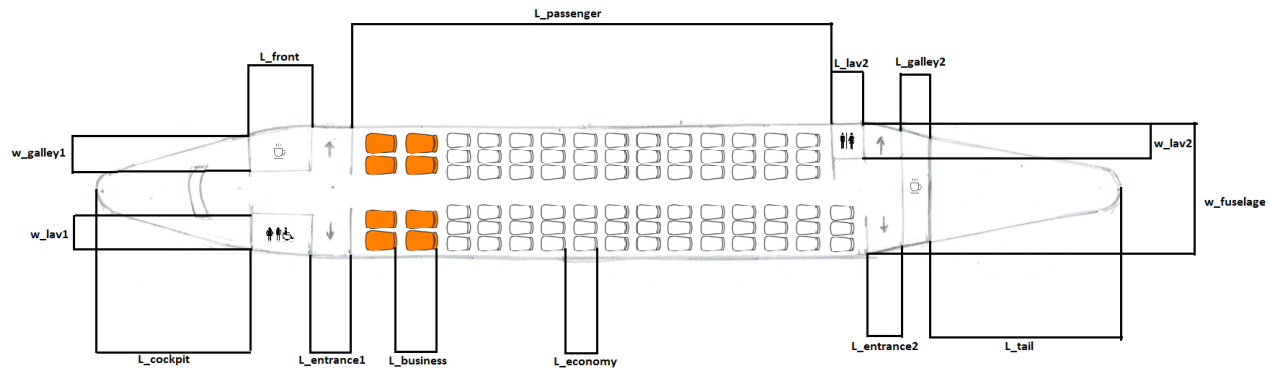


Figure B.1: Top view of the fuselage, dimensions in Table 11

Table 11: Dimensions corresponding to the top view [19] shown in Figure B.1

Name	Dimension[m]	Name	Dimension[m]	Name	Dimension[m]
L-cockpit	4	L-front	1.5	L-economy	0.7875
L-entrance1	1	L-passenger	11.5	L-lav2	1
L-enterance2	1	L-business	1.02	w-lav2	0.9
L-galley2	0.75	L-tail	5.9	w-lav1	1.05
W-galley1	0.75	w-fuselage	3.5		

Name	Dimension (m)
R_H2	0.8-1.54
h_aisle	2
h_cargo	1.63
w_aisle	0.485/0.79
w_seat	0.458/0.61
w1_cargo	3.16
w2_cargo	2.34
t_layer	0.18
h_storage	0.25
w_storage	0.45
t_skin	0.12

Table 12: Cross section dimensions [19], Figure B.2

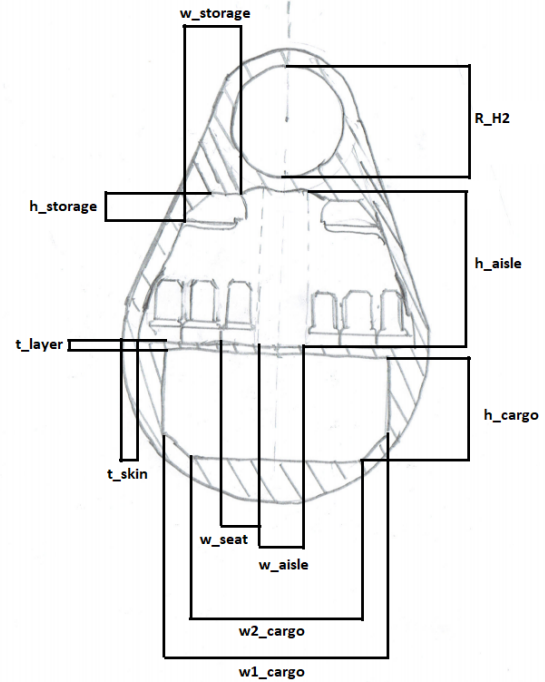


Figure B.2: Cross section of the fuselage with dimensions shown in Table 12

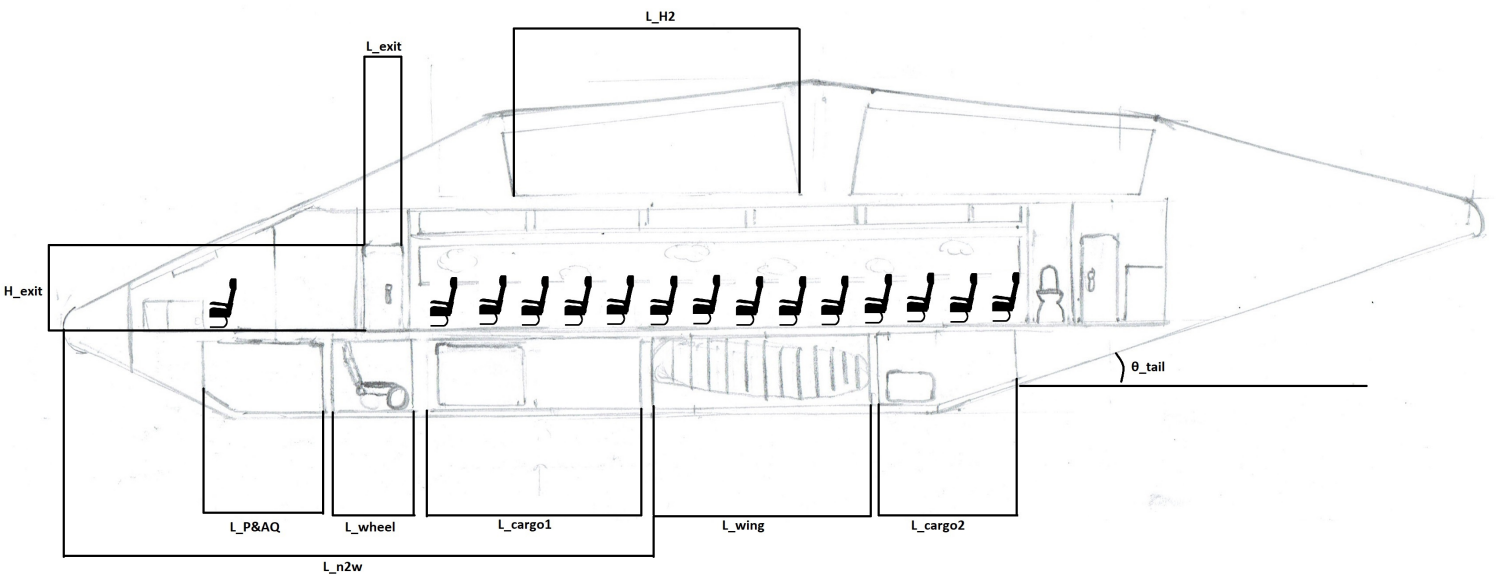


Figure B.3: Side view of the fuselage with dimensions shown in Table 13

Table 13: Dimensions corresponding to the side view [19] as shown in Figure B.3

Name	Dimension (m)	Name	Dimension (m)	Name	Dimension
L_P&AQ	2	L_wheel	1.5	$\theta_{tail}$	19°
L_cargo1	3.10	L_wing	4.5	L_n2w	12.9 m
L_cargo2	2	L_H2	5.5		
H_exit	1.83	L_exit	0.81		

## C Business Case

### C.1 Problem

The airline industry has been growing steadily during the second half of the 20th century and has been increasing at different rates ever since. The total number of passengers yearly is 4.1 billion and is predicted to double before 2037 [45]. Profits in this industry are among the thinnest [46] in the world and most of the costs are spent on fuel which is also one of the main sources of pollution. The airline industry contributes to 2% of the production of greenhouse gases worldwide. However, while many new green alternatives are being found for other industries, airlines are predicted to increase their negative impact unless regulations are introduced by governments. “While “only” 2-3% [47] of worldwide emissions come from flying, according to Roland Berger, this could reach 10% by 2050 or even 24% if other sectors get cleaner faster”. For these reasons, the main focus point of recent environmental summits has been that of discussing and finding a clean alternative for clean-air transportation. The International Civil Aviation Organization (ICAO) has set a goal to keep the rate of CO<sub>2</sub> production steady and doing so by adopting clean solutions (i.e. electric batteries and hydrogen). So far, and in short term prospects, electric aviation will not be as profitable as current solutions are, however it is a key role for the government to address the environmental issue. Starting to explore the field is as important as finding economic benefits and it is said to be just a matter of time before clean solutions, such as batteries and hydrogen fuel, will overcome their kerosene-based counterparts. To sum up, the problem that is being solved by the proposed design is not only transportation but also to reduce the environmental footprint of current air mobility systems. Starting implementing these green alternatives is one of the milestones for making such alternatives as profitable, if not more, as the current solutions, while having a positive impact on the environment.

### C.2 Solution

The solution proposed is that of a hydrogen-powered aircraft deployed by a new airline working specifically with green technology. All flights provided are emission-free and will not produce any amount of CO<sub>2</sub>. Hydrogen was adopted as a fuel because its whole process of harvesting and consumption still has a much lower environmental impact when compared to other “clean” energy sources such as batteries, in addition to other reasons regarding technical feasibility and efficiency. Many demands regarding a fast, efficient and green air transportation system have been raised, not only by governments and summits, but most importantly by people in society. For this reason the solution proposed will be of great value, despite initially requiring higher prices compared to current alternatives. The aircraft will be similar to current mid-long-range planes such as city hoppers and will be

operational in all the main airports of the selected target region. All design choices have been made taking into account 2 main aspects: sustainability and costs with priority given to the first as long as costs wouldn't be higher than earnings. This aircraft would be one of its kind as it would be the first operational passenger plane without CO<sub>2</sub> emissions. More details on the aircraft that will be employed are that it will require a runway length of 1500 m and will have a flying range of 1000 km with diversion capabilities of 10% both in flying distance and time. This is about one-third of the range of an Airbus A320 (3200km). However, further research is predicted to reduce the gap in the upcoming years. Moreover, ticket prices are generally not directly proportional to the distance travelled per passenger motivating this relatively shorter range. This aircraft is aimed at regional and inter-regional travel making 1000 km of range a good starting point when also considering a cruise speed of 550 km/h.

### C.3 Value

As aforementioned, the current contribution of CO<sub>2</sub> emission brought about by the whole airline sector is between 2-3% and considering its slow adaption to cleaner alternative, this number may be 10 times higher in the upcoming 30 years. According to [48] the average number of travel flights per day in 2019 was 167000 flights. We estimated that having one single airline deploying a fleet of 100 of the proposed aircraft, may lead to an immediate reduction of 0.2-0.5% of CO<sub>2</sub> emissions. This is a significant initial contribution and once proven to be safe and efficient, in addition to the technological improvement of hydrogen storage as well as contribution to governmental incentives, it may even turn out to become the most profitable in the future. The value provided would also be one of its kind when compared to the competition, in fact, in the short term, no airline has a concrete plan of flying emission-free whilst this new proposed airline is set never to release any polluting gas since its genesis. Besides, instead of producing and selling the proposed aircraft, operating an airline only employing zero-emission aircraft and allowing passengers to travel carbon-free, is an important step towards accountability and focus to make the technological progress steady. In fact, unlike our competitors, TITAN aims to offer clean travelling within regional and inter-regional distances rather than just an emission-free plane. It is our mission to empower and allow the global population of flying with a neutral environmental footprint and we believe that to be possible by directly offering such service to the passengers instead of waiting for outside airlines, mainly interested in profit, to acquire the aircraft we are proposing. To sum up, despite having to initially sacrifice an improvement in profitability, the value that such solution brings lies on different perspectives, the most important being the environmental and societal ones.

### C.4 Market size and future development

A market analysis has been carried out on the current travel and air mobility sector. That is indeed the target for the proposed aircraft as it is aimed to initially introduce a green alternative and eventually give proof that flying without emission can be profitable so that other airlines will adopt such solutions. A comprehensive market analysis has been carried out: first, the number of possible passengers who already fly with kerosene-fueled airplanes has been looked into. This is shown in Table 14.

Regions:	Travelers:
European Union	636,860160
Europe, Central Asia	1,082,810020
East Asia & Pacific	1,363,172030
South Asia	189,225470
Middle East, North Africa	263,132440
Sub-Saharan Africa	63,070540
North America	978,402000
Latin America, Caribbean	292,832220

Table 14: Passengers per region [49]

Subsequently, the distribution of passengers income per region is determined (Table 15 and [50]) as the proposed aircraft will initially have relatively higher manufacturing and operational costs leading to a higher ticket price compared to common airlines.

Income bracket	Threshold (\$/year)	Amount of travelers (1000)
High income (dark red)	>12,375	2,448,980.79
Upper-middle income (light red)	3,996-12,375	1,409,279.23
Lower-middle income (light blue)	1,026-3,995	355,942.96
Low income (dark blue)	<1,026	18,441.75

Table 15: Passengers per income bracket [49] in 2018

The proposed solution mostly concerns people who are worried about their environmental impact hence an analysis on climate awareness per region has been carried out, as can be found in [51]. Besides, a projection of future population and income has been looked into so that we could have a rough estimation of future prospective and also considering that such aircraft will require few years before it will be prototyped, tested and manufactured at scale. Looking from a regional perspective, the income of the population has a big influence on the amount of air travel in a region. Therefore, Africa should only be a minor interest as a market, although the population will increase fast in the future. Europe, Northern America and Oceania are already a big market due to the high income, although they do not think climate change is a serious threat. But if the possibility is there, due to the high income, the population will probably not mind paying a small extra amount. Also, in 2030 they will still have the largest amount of travellers in the world, so these regions will remain a big interest for the market. The Latin-American population will be open to pay extra to fly with a climate-neutral plane. This means that the Latin-America market has a high potential. The Middle East has as many inhabitants as Latin America and the income is also comparable, but there is too little information for climate awareness to make a guess therefore it is not very promising to choose this as a potential market. Lastly, Asia is the biggest growing market of them all, due to the increase in wealth. They have a relatively low awareness of climate change, but due to the number of people, it is a big market that has to be considered. [45] [52] [53] [54]

## C.5 Competition and possible partners

Despite being one of the few airlines without gas emission whatsoever, it is still important to determine competitors and possible partnerships. Given the interest of Airbus in starting to develop transportation, they have less and less of an environmental footprint [55]. They may be assumed to be a possible partner. However, it is important to look into their main competitor: Boeing. Airbus seems to be focusing on developing new technologies to tackle climate change. According to their website, they believe that existing technologies will not achieve the ambitious goals set by the legislators/agreements. Therefore there is the need for new propulsion systems and energy sources [56]. Boeing seems to focus on reducing fuel consumption, (partly) because they don't believe in the successful application of hydrogen fuel. It seems they are trying to improve existing concepts to improve efficiency, with, for example, the help of big data [57]. The success of such a partnership is strongly dependent on the airlines' interest in the environment. Some airlines are more interested in environmentally friendly measures than others. A few airlines who are known for their interest are EasyJet, Ryanair, Cape Air and LoganAir [58]. Similar to EasyJet, Ryanair has a clear plan for reducing carbon emissions in the future. Although they are not as invested in new technologies as EasyJet yet, they already call themselves Europe's cleanest airline and offer carbon offsetting to their customers [59]. Cape Air mostly covers the United States. Here, no environmental initiatives were found, but having an interest in flying electric is also mentioned. [58]. Outside Europe and the United States, not many airlines seem to be potential competitors. A few big airlines are chosen to analyze, such as China Airlines and Air India. China Airlines focuses mainly on reduction and improvement of existing methods and systems, rather than investing in new aircraft. It seems they are not exactly on track to go for zero-emissions (yet). Air India does not have any environmental initiatives on their website [60], except from a standard policy. Although South America is interesting considering income and climate awareness, it does not seem to be the right market for the concept design right now. With most airlines struggling financially and no financial backing being expected by the current political situation, an investment into new technologies does not seem feasible at the moment.

## C.6 Competences and Complexity

The reference aircraft is an Airbus A320neo. Three hydrogen concepts had been compared to the baseline aircraft. The increase in block-energy required for the hydrogen concept compared to baseline aircraft was lowest for the concept in which the hydrogen tanks were stored on top of the aircraft. For this concept, the block-energy required due to the mass effect is actually 3 percent less than required for the baseline aircraft. However, the combination of Aerodynamic and boil-off effects cause the overall effect at the block-energy to be 6 percent higher. [1] Hydrogen tanks and a new hydraulic system to distribute fuel to the motors are the main differences when comparing the proposed aircraft to the common airliners produced by Boeing and Airbus. Moreover, the absence of passenger windows, substituted by cameras, indicates an additional degree of difference. Given the already complex build, tapered wings have been preferred to elliptical wings, despite being slightly less efficient, because of the lower prices of production and maintenance as well as a larger wing stub (about 10%) for more room for the main landing gear and less weight which overall counterbalances the slightly higher efficiency of elliptical wings [48]. All changes applied will require new competencies in manufacturing and more importantly in operating and in the costs of the aircraft. All redesigns and changes compared to typical aircraft have been chosen to address the efficiency and net profitability of operating an airline employing only the proposed hydrogen-fueled design. Hydrogen tanks will increase the aerodynamic drag hence lowering the efficiency during flight, of about 6% according to [1]. The redesign of the hydraulic system will have no impact over the efficiency of the plane, however, will require to adapt the manufacturing process of the whole aircraft. Furthermore, the absence of windows will help improve the aerodynamics hence leading to regain some flight efficiency. Cameras will be installed to allow passengers and pilots to observe the outside from the fuselage, required for safety by all aviation regulatory agencies. The production of

the aircraft is not strictly dependent on new technologies, however being first of its kind, technological development will be crucial to further improve the efficiency, not as high as for common airliners yet.

## C.7 Uncertainty

The main uncertainties for the production of our proposed airplane are the functionality of hydrogen tanks on top of the aircraft. This is not because there are better ways to position the tanks, but mainly because each possible solution has its own drawbacks and the best solution has been chosen. Testing will be a significant component; in fact, new testing procedures shall be designed given the originality of the aircraft. As already stated, current technologies allow the aircraft to be possible, making it not immediately dependent on ongoing R&D, however, the main aircraft manufacturers still haven't employed hydrogen as an engine fuel and no tangible proof of concept has been present in the market yet. As mentioned earlier, customer demand is significant in particular regions that are intended to target, hence requests for adopting this new clean mean of transport is certain and making the whole concept economically feasible.

## C.8 Costs and returns

A financial analysis has been carried out by referring the income statement of the SouthWest Airline Co. [61] and the KLM Royal Dutch Airlines [62] of the past 4 years. According to [63] only 60% of airline revenue comes from selling flight tickets to passengers and the remaining 40% revenue source is from selling frequent-flier miles to credit card companies and other travel partners like hotels and car rental agencies. It is also stated that business tickets can represent up to 75% of a single flight revenue. Moreover, according to the official KLM website [64], in 2019, with a fleet of 115 planes, a total number of 35.1 million passengers was transported. In light of the above mentioned data, a fleet of 100 planes has been used to get insight into a future scenario for costs and profits of an airline based on the aircraft proposed by this paper. Each plane has 8 business seats and 75 economy seats. Most of operational costs are considered to be the same as for all airlines, however, adjustments have been made on the ticket prices; they are higher due to the lower efficiency of hydrogen planes, the tax returns, they are lower thanks to the incentives of the government and the manufacturing and maintenance costs. Furthermore, the ticket price will be higher due to the production of a new plane and the specific maintenance required for this new type of aircraft. The results can be seen in Table C.4.

	2021	2022	2023	2024	2025
<b>Sales/Revenue</b>	30,000	31,500	33,075	34,728	36,465
<b>Sales Growth</b>		5%	5%	5%	5%
<b>Assets</b>					
<b>Operational costs</b>	-23,000	-23,000	-24,000	-24,000	-24,000
<b>Depreciation &amp; Amortization Expense</b>	-3,500	-3,750	-4,000	-4,250	-4,500
<b>Gross Income</b>	3,500	4,500	5,075	6,478	7,965
<b>SG&amp;A Expense</b>	-1,500	-1,750	-2,000	-2,250	-2,500
<b>Earnings before interest and taxes</b>	2,000	2,750	3,075	4,228	5,465
<b>Interest Expense</b>	-750	-750	-750	-750	-750
<b>Pretax Income</b>	1,250	2,000	3,325	3,478	4,935
<b>Income Tax</b>	100	100	100	100	100
<b>Net Income</b>	1,150	1,900	3,225	3,378	4,835

Figure C.4: Future scenario income statement 2021-2025. All numbers are in million €

Given the above estimated yearly incomes and expenses, a first indication of flight tickets may be given, ranging from 200-300€ depending on the seat option (business or economy) and the flight range. A 5% sales growth per year for the first 5 year has been assumed which is slightly higher to the typical 2-3% of common airlines because of such an innovative concept for passengers mobility. In addition, an estimation of the breakeven times can be derived. According to [65] the average price of a McDonnell Douglas MD-90 is of about 48m\$, with a capacity of 80-135 passengers and a 4500km range, considering that the aircraft that is proposed particularly innovative and there has been little manufacturing experience regarding hydrogen powered airplanes, the average price is set to produce such aircraft to be around 75-95m€. Such prices have been estimated on current R&D investments in the aircraft market. Most production work on the aircraft is specifically aimed at the redesign of the fuel system and the addition of the hydrogen storage tank. Other changes applied to the aircraft, when compared to Boeing or Airbus, are not as significant as the new implementations required for the energy storage, hence only a 20% increase in manufacturing costs has been considered. Referring to the net income of table C.4 and the constant

growth rate, as well as the costs required to deploy additional planes to accommodate the growth, breakeven is supposed to be reached within 10-11 years from the first operational year.

## C.9 Times

Referring to existing airplanes [66], the whole process of design, testing and manufacturing usually takes 2-4 years. This process is very intensive, expensive and requires various iterations and for such reasons it is critical for the success of the design and particularly time consuming. Arising delays are likely to occur, especially if a new design is proposed, requiring new processes to be adopted. For all the reasons mentioned above, about 5 years are expected from the first design iteration to flying commercially and with certified licensing from each of the regions where such aircraft will be deployed.

## C.10 Risks

The main risks that may jeopardize the success of this new airliner are both in terms of technicality and profitability. First of all it is required that the proposed design is feasible and safe; failing to build such an aircraft would jeopardize the idea of offering emission-free flights while still gaining profit. In addition, safety is another important factor. Being licensed to fly is a very time consuming process and many features have to be accepted by the governmental standards. Taking too much time in the validation process would put the aircraft at risk because delays are not well seen by creditors and investors and often end up with high unexpected costs. Once the aircraft is operating, it is important that passengers are adopting it instead of other polluting transportation means and that maintenance and operational costs are lower than the gross profit. This is again crucial for the aircraft to survive in the current market and to motivate other airlines in adapting clean solutions that are also still profitable.

## D Group contribution

<b>J. Leeftink</b>	Landing gear design
<b>M. Lamers</b>	Performance
<b>R. Koenderink</b>	Fuselage design & mass estimation
<b>H. Jekel</b>	Group leader, stand-by help
<b>D. Tjokrosetio</b>	Stabilizer design
<b>N. Jansen</b>	Engine design & mass estimation
<b>S. E. F. Ismail</b>	Business case
<b>M. Schnatterer</b>	Wing design

# Conceptual hydrogen aircraft



**1000 km**

A regional airliner with a range of 800 to 1000 km.

**550 km/h**

Cruising on 9000 m at 550 km/h.

**9520 kg**

The aircraft transports crew, passengers with luggage and cargo.

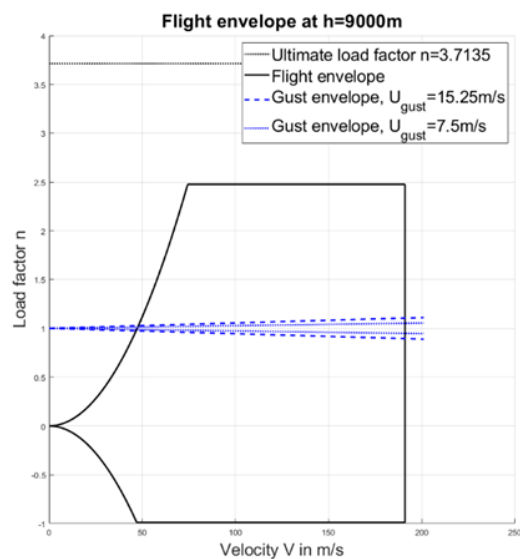
**83 seats**

8 business and 75 economy seats.

**€200 per ticket**

Estimated ticket prices starting from €200.

To reduce and even eliminate carbon emissions of aircraft, other ways of propelling are needed. This climate neutral airplane flies on direct combustion of hydrogen. With a necessary runway length of 1425 m in normal conditions, this regional airliner can take-off and land at most airports.



Wing span	33.5 m
Fuselage length	27 m
Maximum take-off mass	24500 kg
Maximum fuel mass	840 kg
Power per engine	3.125 MW
Power required during cruise	1.6 MW
Time to reach cruising altitude	15 min 50 s
Take-off runway length	1260 m
Landing runway length	1425 m

Ideal customers would be North-American and European airlines, such as Ryanair, Cape Air, EasyJet and Logan Air, which offer many regional flights. The estimated price of the aircraft is 95 million euros. Breakeven is expected to be reached within 11 years from

Concept to operation	5 years
Breakeven	11 years
Costs	€95.000.000
Estimated sales growth	5% per year

Group 7: J. Leeftink(s2188295), M. Lamers (s1935429), R. Koenderink (s2139995), H. Jekel (s1802178), D. Tjokrosetio (s2089688), N. Jansen (s2184745S), E. Ismail (s2169851), M. Schnatterer (s2621150).  
Source: J. Leeftink, M. Lamers, R. Koenderink, H. Jekel, D. Tjokrosetio, N. Jansen., S. E. F. Ismail, and M. Schnatterer, "Conceptual design of a climate neutral regional airliner," January 2020.

12-01-2020

UNIVERSITY  
OF TWENTE

Figure E.5: Fact sheet